

CHARACTERIZATION OF DEVONIAN BLACK  
SHALE DEPOSITIONAL ENVIRONMENTS AND  
DIAGENETIC/CATAGENETIC PROCESSES USING  
NITROGEN ISOTOPES AND OTHER GEOCHEMICAL  
PROXIES: OHIO SHALE, EASTERN KENTUCKY

By

BRICE AARON OTTO

Bachelor of Science in Geology

University of Tulsa

Tulsa, Oklahoma

2013

Submitted to the Faculty of the  
Graduate College of the  
Oklahoma State University  
in partial fulfillment of  
the requirements for  
the Degree of  
MASTER OF SCIENCE  
July, 2015

CHARACTERIZATION OF DEVONIAN BLACK  
SHALE DEPOSITIONAL ENVIRONMENTS AND  
DIAGENETIC/CATAGENETIC PROCESSES USING  
NITROGEN ISOTOPES AND OTHER GEOCHEMICAL  
PROXIES: OHIO SHALE, EASTERN KENTUCKY

Thesis Approved:

Dr. Tracy M. Quan

---

Thesis Adviser

Dr. James Puckette

---

Dr. Jack Pashin

---

## ACKNOWLEDGEMENTS

I would like to express my deepest gratitude to the faculty members of the Boone Pickens School of Geology, especially my thesis advisor Dr. Tracy Quan for her commitment and mentorship during this thesis process. I would also like to thank my committee members, Dr. Jim Puckette and Dr. Jack Pashin for their advice and guidance over these past two years. Also, I want to thank Patrick J. Gooding and Ryan L. Pinkston at the Kentucky Geological Survey for helping me select, package, and ship samples for this study. I want to also extend a special thanks to Chris Geyer and Keith Rivera for their assistance and knowledge in the geochemistry lab, and everyone else in our geochemistry group.

This research could not have been conducted without the gracious financial support from the National Science Foundation grant NSF-OCE-0961914, fellowships from the Boone Pickens School of Geology, Newfield Exploration, the Hispanic Scholarship Fund, and Marathon Oil Corporation.

Most importantly, I want to thank my mother, Berlinda Padilla-Otto, and my sister, Bailey Otto, for their continuous support. Thank you for everything, for teaching me to never give up on myself, for constantly believing in me even when I may have not, and for always being in my corner. To my father, Michael Otto, I've almost made it. I will love you and miss you always.

Name: BRICE OTTO

Date of Degree: JULY, 2015

Title of Study: CHARACTERIZATION OF DEVONIAN BLACK SHALE  
DEPOSITIONAL ENVIRONMENTS AND  
DIAGENETIC/CATAGENETIC PROCESSES USING NITROGEN  
ISOTOPES AND OTHER GEOCHEMICAL PROXIES: OHIO SHALE,  
EASTERN KENTUCKY

Major Field: GEOLOGY

Abstract:

Research investigating catagenetic alterations of  $\delta^{15}\text{N}_{\text{bulk}}$  values in Devonian shales have shown little correlation between  $\delta^{15}\text{N}_{\text{bulk}}$  profiles and thermal maturities; instead it was concluded that  $\delta^{15}\text{N}_{\text{bulk}}$  values primarily reflect the paleoredox conditions during deposition. Separating inorganic nitrogen (IN) from bulk nitrogen has proven useful to be a useful proxy for characterizing catagenetic alterations because IN, in the form of  $\text{NH}_4^+$ , is released from organic matter (OM) during thermal degradation and fixed by surrounding authigenic clays. Conceptually, three scenarios can exist between bulk and inorganic nitrogen isotopic values at a particular depth: (1)  $\delta^{15}\text{N}_{\text{bulk}} > \delta^{15}\text{N}_{\text{inorg}}$  (positive); (2)  $\delta^{15}\text{N}_{\text{bulk}} < \delta^{15}\text{N}_{\text{inorg}}$  (negative); or (3)  $\delta^{15}\text{N}_{\text{bulk}} \approx \delta^{15}\text{N}_{\text{inorg}}$  (closed). Along with characterizing the paleoredox conditions of the Ohio Shale, our research will also evaluate the driving mechanism responsible for these relationships between  $\delta^{15}\text{N}_{\text{inorg}}$  and the original paleoredox-dependent  $\delta^{15}\text{N}_{\text{bulk}}$  value.

Using  $\delta^{15}\text{N}_{\text{bulk}}$  and TOC as our proxies for oxygen content and preservation of OM, it is possible to evaluate the paleoredox evolution during Ohio Shale deposition at the A. Lowe Heirs KL4-504695 in Pike County, Kentucky. The lower and upper Huron were deposited in predominantly anoxic conditions under the pycnocline, while the middle Huron was deposited under alternating suboxic and anoxic conditions. The Chagrin was predominantly deposited in a suboxic environment within the pycnocline. The Cleveland equivalent was deposited proximal to upwelling conditions but not within the oxygen minimum zone. The relationship between  $\delta^{15}\text{N}_{\text{bulk}}$  and  $\delta^{15}\text{N}_{\text{inorganic}}$  values is dependent on paleoredox conditions, clay contents, degradation-recondensation processes, and diagenetic and catagenetic processes. Negative crossover profiles, associated with anoxic intervals, suggests that isotopic buffering is occurring along with an observed inversion of normal fractionation kinetics during thermal degradation of OM, and the preferential uptake of heavy  $^{15}\text{NH}_4^+$  by authigenic clays. Positive crossover profiles, associated with suboxic conditions, suggest that normal isotopic fractionation kinetics prevails, releasing isotopically light  $^{14}\text{NH}_4^+$  during the thermal degradation of OM. Closed intervals are indicative of compartmentalization and isotopic equilibrium exchange between stationary OM and circulating  $\text{NH}_4^+$  pools.

## TABLE OF CONTENTS

Chapter	Page
I. INTRODUCTION.....	1
The relationship: marine nitrogen cycle, sedimentary $\delta^{15}\text{N}_{\text{bulk}}$ values, and redox conditions.....	3
Diagenetic and catagenetic processes.....	8
II. STUDY SITE.....	11
Divisions of the Ohio Shale.....	11
Stratigraphic framework.....	14
Acadian Orogeny.....	18
Eustasy.....	20
Controls of organic carbon in the central Appalachian Basin.....	22
III. METHODOLOGY.....	24
Stable isotopic compositions and elemental concentrations.....	24
Laboratory procedures.....	26
Calibration, quality control, and statistical analysis.....	27
IV. RESULTS.....	30
Geochemical results: lower Huron Member.....	30
Geochemical results: middle Huron Member.....	31
Geochemical results: upper Huron Member.....	31
Geochemical results: Chagrin Member.....	32
Geochemical results: Cleveland equivalent Member.....	32

Chapter	Page
V. DISCUSSION .....	35
Paleoredox evolution and depositional model of the Ohio Shale .....	35
Other geochemical proxies .....	38
Validity of depositional environment interpretations .....	40
Relationship between $\delta^{15}\text{N}_{\text{bulk}}$ and $\delta^{15}\text{N}_{\text{inorg}}$ .....	41
Implication of negative ( $\delta^{15}\text{N}_{\text{bulk}} < \delta^{15}\text{N}_{\text{inorg}}$ ) crossover profiles .....	42
Implication of positive ( $\delta^{15}\text{N}_{\text{bulk}} > \delta^{15}\text{N}_{\text{inorg}}$ ) crossover profiles .....	43
Implication of closed ( $\delta^{15}\text{N}_{\text{bulk}} \approx \delta^{15}\text{N}_{\text{inorg}}$ ) intervals .....	45
V. CONCLUSIONS .....	47
Recommendations .....	49
REFERENCES .....	50
APPENDIX I .....	69
APPENDIX II .....	71

## LIST OF TABLES

Table	Page
1. Minimum, maximum, average, and standard deviation values for $\delta^{15}\text{N}_{\text{bulk}}$ (‰), $\delta^{15}\text{N}_{\text{inorg}}$ (‰), TN (wt. %), IN (wt. %), $\delta^{13}\text{C}_{\text{org}}$ (‰), TOC (wt. %), and $\text{C}_{\text{org}}/\text{TN}$ values for the lower Huron Member.....	30
2. Minimum, maximum, average, and standard deviation values for $\delta^{15}\text{N}_{\text{bulk}}$ (‰), $\delta^{15}\text{N}_{\text{inorg}}$ (‰), TN (wt. %), IN (wt. %), $\delta^{13}\text{C}_{\text{org}}$ (‰), TOC (wt. %), and $\text{C}_{\text{org}}/\text{TN}$ values for the middle Huron Member.....	31
3. Minimum, maximum, average, and standard deviation values for $\delta^{15}\text{N}_{\text{bulk}}$ (‰), $\delta^{15}\text{N}_{\text{inorg}}$ (‰), TN (wt. %), IN (wt. %), $\delta^{13}\text{C}_{\text{org}}$ (‰), TOC (wt. %), and $\text{C}_{\text{org}}/\text{TN}$ values for the upper Huron Member.....	32
4. Minimum, maximum, average, and standard deviation values for $\delta^{15}\text{N}_{\text{bulk}}$ (‰), $\delta^{15}\text{N}_{\text{inorg}}$ (‰), TN (wt. %), IN (wt. %), $\delta^{13}\text{C}_{\text{org}}$ (‰), TOC (wt. %), and $\text{C}_{\text{org}}/\text{TN}$ values for the Chagrin Member.....	32
5. Minimum, maximum, average, and standard deviation values for $\delta^{15}\text{N}_{\text{bulk}}$ (‰), $\delta^{15}\text{N}_{\text{inorg}}$ (‰), TN (wt. %), IN (wt. %), $\delta^{13}\text{C}_{\text{org}}$ (‰), TOC (wt. %), and $\text{C}_{\text{org}}/\text{TN}$ values for the Cleveland equivalent.....	33

## LIST OF FIGURES

Figure	Page
1. Schematic diagram of the various transformations and redox states in the marine nitrogen cycle.....	4
2. Schematic showing the isotopic fractionation and enrichment ( $\epsilon$ ) associated with different marine nitrogen biogeochemical processes with regards to $\delta^{15}\text{N}$ .....	5
3. Schematic showing the relationship between bulk sedimentary $\delta^{15}\text{N}$ values and deep water oxygen concentrations.....	8
4. Location of the A. Heirs Lowe KL4-504695 well, Pike Co. (20-N-84, 2055' FSL, 620' FEL) in eastern Kentucky .....	12
5. Well log including gamma ray and induction curves for the A. Lowe Heirs KL4-504695 in Pike County, Kentucky.....	13
6. Generalized stratigraphic column for eastern Kentucky.....	14
7. Tectonic setting during the late Devonian Acadian orogeny and the impending collision of the Virginia promontory responsible for the 3 <sup>rd</sup> Acadian tectophase...18	18
8. Schematic diagram showing the deposition of black shale, gray shale, and clastic sequences from the Middle to Late Devonian .....	19
9. Late Devonian paleogeographic map of North America showing the Appalachian Basin .....	22
10. Bulk nitrogen isotope ( $\delta^{15}\text{N}_{\text{bulk}}$ ), inorganic nitrogen isotope ( $\delta^{15}\text{N}_{\text{inorg}}$ ), organic carbon isotope ( $\delta^{13}\text{C}_{\text{org}}$ ), total organic carbon (TOC), inorganic nitrogen (IN), and $\text{C}_{\text{org}}/\text{TN}$ profiles for the individual members of the Ohio Shale: lower Huron, middle Huron, upper Huron, Chagrin, and Cleveland equivalent members.....	34
11. Schematic diagram using $\delta^{15}\text{N}_{\text{bulk}}$ and TOC as proxies for oxygen concentration and OM preservation. ....	36



Figure	Page
12. Synthetic depositional model during the deposition of the lower Huron, middle Huron, upper Huron, Chagrin, and Cleveland equivalent members .....	37
13. Schematic diagram explaining the diagenetic/catagenetic processes and mechanisms responsible for negative and positive crossover profiles .....	44
14. Schematic diagram illustrating isotopic equilibrium exchange between stationary OM and circulating $\text{NH}_4^+$ within a compartmentalized interval.....	46

## CHAPTER I

### INTRODUCTION

Characterizing the depositional environment of organic-rich shales has long been of interest for evaluating source rock and reservoir potential. The quality of organic matter (OM) preserved in shales varies immensely, depending on the amount of biological activity and the environment of deposition (Hunt, 1979). The Ohio Shale of eastern Kentucky is a marine black shale of Devonian age that is equivalent to other black shale formations of the North American craton spanning from New York and as far west as New Mexico (Ettensohn, 1992). The Ohio Shale is heterogeneous and is subdivided into a series of members and submembers: the lower Huron, middle Huron, upper Huron, Chagrin and Cleveland shales (Provo *et al.*, 1978). Pioneering work by Rich (1951) was the first to suggest that the Upper Devonian bituminous shales of east-central United States were deposited in poorly aerated waters in the deepest unfilled parts of the Appalachian geosyncline, and encroached upon by clinoform deposits. Originally, shale deposition in deep marine environments was thought to be controlled by water stratification and the vertical position of the pycnocline; however, black shale depositional environments have proven to be more dynamic. Characterizing the specific paleoredox conditions of black shale depositional environments has provided the intellectual merit for geochemical studies in the Ohio Shale and its individual members

(e.g. Ettensohn *et al.*, 1988; Robl and Barron, 1988; Calvert *et al.*, 1993; Rimmer, 2004; Rimmer *et al.*, 2004; and Perkins *et al.*, 2008). Although multiple depositional environment studies have been conducted on the Ohio Shale and its equivalents, research has yet to be performed on the utility of nitrogen isotopes ( $\delta^{15}\text{N}_{\text{bulk}}$ ) as a proxy for paleoredox conditions in this formation.

Hoering (1955) was the first to use stable nitrogen isotopic delta values ( $\delta^{15}\text{N}$ ) to characterize natural substances (e.g. plants, animals, coals, oils, and minerals). Other studies were then performed to characterize nitrogen isotopic values and isotopic fractionation related to non-marine and marine biogeochemical processes (e.g. Delwiche and Steyn, 1970; Wada *et al.*, 1975; Wada and Hattori, 1976; Minagawa and Wada, 1986; Checkley Jr. and Miller, 1989). Nitrogen isotopes have been used to evaluate sedimentary OM from an isotopic perspective since the 1970s (e.g. Peters *et al.*, 1978; Rau *et al.*, 1987). Subsequent studies using sedimentary  $\delta^{15}\text{N}_{\text{bulk}}$  have evaluated paleoredox conditions (e.g. Macko, 1981; Rau *et al.*, 1987; Macko, 1989; Holmes *et al.*, 1996; Lehmann *et al.*, 2002; Junium and Arthur, 2007; Quan *et al.*, 2008; Quan and Falkowski, 2009; Godfrey and Glass, 2011), changes that occur as particulate OM descends through the water column (e.g. Altabet and Francois, 1994; Robinson *et al.*, 2012), and burial diagenesis within a few meters of the water-sediment interface (e.g. Müller, 1977; de Lange, 1992; Freudenthal *et al.*, 2001; Lehmann *et al.*, 2002). However, majority of these studies evaluated immature sediments that have not undergone thermal maturation during catagenesis. Research investigating catagenetic alterations of  $\delta^{15}\text{N}_{\text{bulk}}$  values in Devonian shales (Rivera *et al.*, 2015) have shown little correlation between  $\delta^{15}\text{N}_{\text{bulk}}$  profiles and thermal maturities; instead it was concluded that  $\delta^{15}\text{N}_{\text{bulk}}$  values

primarily reflect the paleoredox conditions during deposition. Previous studies that separated inorganic nitrogen (IN) from bulk samples have proven IN to be useful for characterizing catagenetic alterations within an unconventional system during thermal maturation of OM (Williams *et al.*, 1989; Williams and Ferrell Jr., 1991; Williams *et al.*, 1992; Williams *et al.*, 1995). This is because IN, in the form of aqueous ammonium ( $\text{NH}_4^+$ ), is generated during the thermal degradation of OM and fixed by surrounding clays (Compton *et al.*, 1992; de Lange, 1992; Schroeder and Ingall, 1994; Krooss *et al.*, 1995; Littke *et al.*, 1995; Mingram *et al.*, 2003; Jia, 2006; Schimmelmann and Lis, 2010). Conceptually, three scenarios can exist between bulk and inorganic nitrogen isotopic values at a particular depth: (1)  $\delta^{15}\text{N}_{\text{bulk}} > \delta^{15}\text{N}_{\text{inorg}}$ , (2)  $\delta^{15}\text{N}_{\text{bulk}} < \delta^{15}\text{N}_{\text{inorg}}$ , or (3)  $\delta^{15}\text{N}_{\text{bulk}} \approx \delta^{15}\text{N}_{\text{inorg}}$ . Along with characterizing the paleoredox conditions of the Ohio Shale, our research will also evaluate the driving mechanism responsible for these relationships between  $\delta^{15}\text{N}_{\text{inorg}}$  and the original paleoredox-dependent  $\delta^{15}\text{N}_{\text{bulk}}$  value. To support our research,  $\delta^{15}\text{N}_{\text{bulk}}$ ,  $\delta^{15}\text{N}_{\text{inorg}}$ , organic carbon ( $\delta^{13}\text{C}_{\text{org}}$ ) isotope analyses, and total nitrogen (TN), IN, and total organic carbon (TOC) elemental concentrations will be measured.

### *1.1 The relationship: marine nitrogen cycle, sedimentary $\delta^{15}\text{N}_{\text{bulk}}$ values, and redox conditions*

The nitrogen cycle is one of the most complex and diverse biogeochemical cycles in the marine realm. The marine nitrogen cycle involves a range of nitrogen compounds and a variety of redox states (Fig. 1) as transformations are undertaken by marine organisms as part of their metabolism, either to gain energy for growth or to synthesize structural components (Gruber, 2008; Mulholland and Lomas, 2008). The

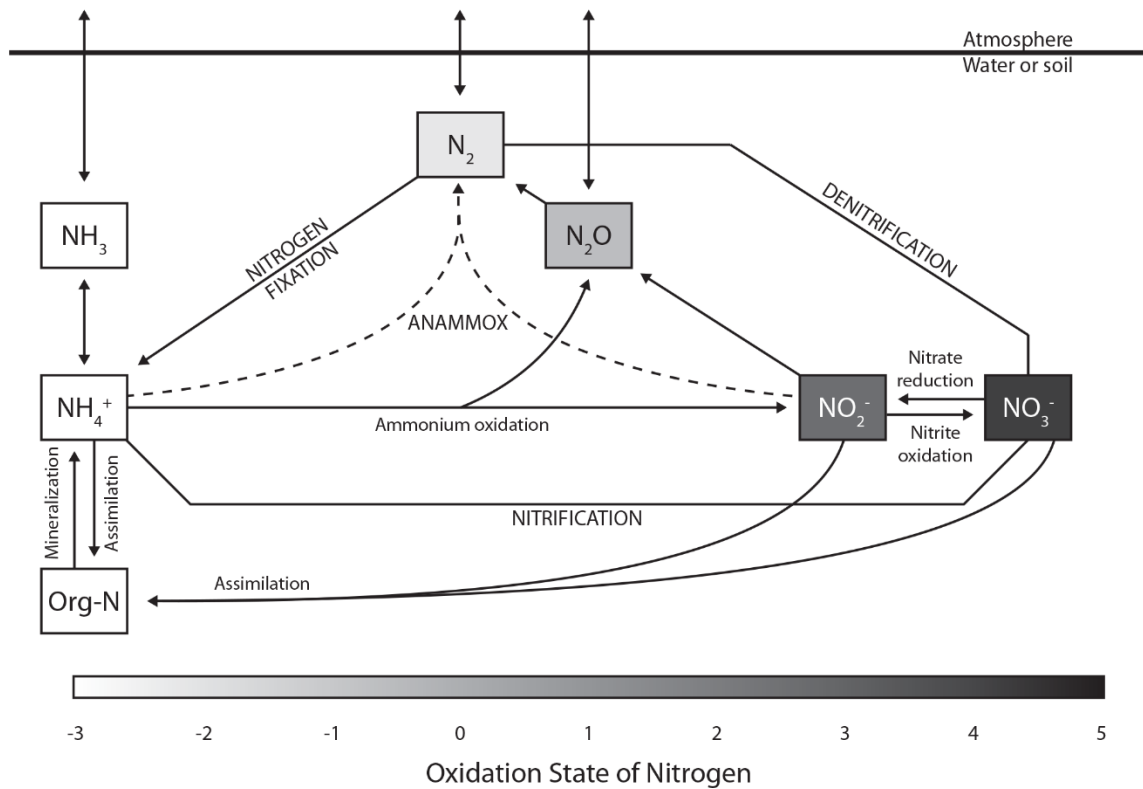


Figure 1. Schematic diagram of the various transformations and redox states of nitrogen in the marine nitrogen cycle (Modified from Karl and Michaels, 2001)

main processes of the biologically driven marine nitrogen cycle on geological time scales are fixation, nitrification, denitrification, and anammox (anaerobic ammonium oxidation). Each of the aforementioned reactions predominates under specific redox conditions and is characterized by unique isotopic fractionation factors ( $\alpha$ ) (Fig. 2). When organisms assimilate the surrounding nitrogen into their body mass, the  $^{15}N$  content of the nitrogen source will be imprinted in the OM that is eventually deposited on the sea floor and incorporated into the sedimentary record (Minagawa and Wada; 1986; Altabet and Francois, 1994; Robinson *et al.*, 2012).

Nitrogen fixation, the reduction of atmospheric  $N_2$  into fixed nitrogen, is the process responsible for nitrogen input into the marine system. Dissolved atmospheric  $N_2$  is the most abundant form of nitrogen in the ocean; however, it is not bioavailable to

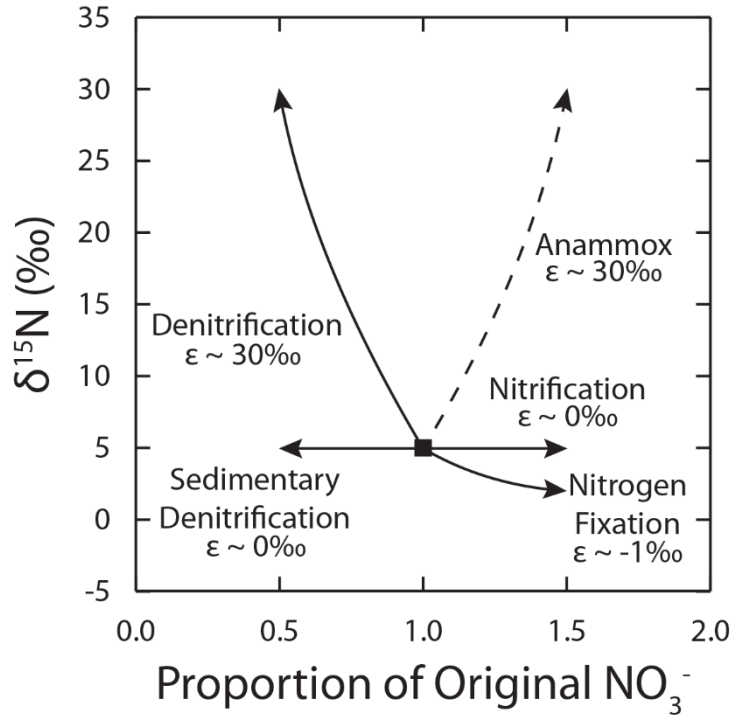


Figure 2. Schematic showing the isotopic fractionation and enrichment ( $\epsilon$ ) associated with different marine nitrogen biogeochemical processes with regards to  $\delta^{15}\text{N}$  (Modified from Montoya, 2008)

most organisms (Karl and Michaels, 2001; Galbraith *et al.*, 2008; Gruber, 2008). The reduction of atmospheric nitrogen to fixed nitrogen via nitrogen fixation allows other nitrogen consuming organisms to use the once unavailable dissolved  $\text{N}_2$  (Eq. 1.1).



Nitrogen fixation is the predominant processes in anoxic conditions since other nitrogen cycle processes are less prominent. Nitrogen fixation occurs with little isotopic fractionation (Delwiche and Steyn, 1970; Wada *et al.*, 1975; Minagawa and Wada, 1986; Carpenter *et al.*, 1997; Beaumont *et al.*, 2000; Galbraith *et al.*, 2008) (Fig. 2), leaving residual combined nitrogen isotopically depleted. This results in low  $\delta^{15}\text{N}$  values upon assimilation into OM and transfer into the sedimentary record.

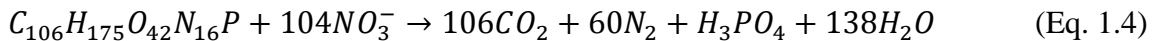
Nitrification is the process that links the most reduced (ammonium) and most oxidized (nitrite and nitrate) forms of nitrogen. Nitrification involves the aerobic

oxidation of  $\text{NH}_4^+$  in a two-step process by: oxidation of ammonium into nitrite (Eq. 1.2) by one consortium of bacteria, and nitrite into nitrate (Eq. 1.3) by another (Teske *et al.*, 1994; Gruber, 2008; Ward, 2008; Casciotti *et al.*, 2011).



Nitrification is the predominant process in oxic conditions and is characterized by little isotopic fractionation (Delwiche and Steyn, 1970; Wada, 1980) (Fig 2.); therefore, producing low sedimentary  $\delta^{15}\text{N}_{\text{bulk}}$  values when residual nitrate is incorporated into OM and transported into sedimentary record (Altabet and Francois, 1994; Meckler *et al.*, 2007).

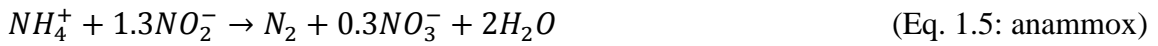
Denitrification is one of the processes responsible for the output of nitrogen from the marine realm. Denitrifiers reduce nitrate to  $\text{N}_2$  via the stoichiometric equation shown in (Eq. 1.4: denitrification) (Gruber, 2008).



Denitrifiers are facultative anaerobes, and under suboxic conditions use nitrate as a terminal electron acceptor (Karl and Michaels, 2001; Devol, 2008). Denitrification is the predominant reaction in suboxic conditions. Increased oxygen concentrations in the water column inhibit the denitrifying enzymes from functioning (Codispoti *et al.*, 2001; Quan *et al.*, 2008; Quan and Falkowski, 2009), but adequate amounts of oxygen must be present to support the production of nitrate (Karl and Michaels, 2001). Incomplete denitrification is characterized by a large isotope effect (Wada *et al.*, 1975) (Fig. 2), leaving residual nitrate enriched in  $^{15}\text{N}$  that is translated into OM and into the sedimentary record

(Meckler *et al.*, 2007; Galbraith *et al.*, 2008; Quan *et al.*, 2008; Quan and Falkowski, 2009; Quan *et al.*, 2013).

Anammox also removes bioavailable nitrogen by combining ammonium and nitrite to form N<sub>2</sub> and nitrate via the equation (Eq. 1.5) proposed by Brunner *et al.* (2013).



Anammox is restricted to suboxic environments because it requires low concentrations of oxygen to oxidize ammonium, but high concentrations inhibit the reaction from taking place (Jetten *et al.*, 2001). Prior to the discovery of the anammox reaction (Mulder *et al.*, 1995), strong enrichments of <sup>15</sup>N in the residual nitrite and sedimentary δ<sup>15</sup>N<sub>bulk</sub> values have been attributed to denitrification alone. Kuypers *et al.* (1995) emphasized the significance of anammox in the ocean and the potential consequences it has on the regional nitrogen budget. Brunner *et al.* (2013) concluded that anammox is characterized by large isotopic fractionation and there is a preferential removal of <sup>15</sup>N from nitrite during the oxidation to nitrate. If denitrification was to occur at the same locale, the fractionation during anammox could be superimposed on the isotopic effects of denitrification, resulting in large sedimentary δ<sup>15</sup>N<sub>bulk</sub> values in OMZs (Brunner *et al.*, 2013).

The non-linear relationship between δ<sup>15</sup>N<sub>bulk</sub> and oxygen concentrations results from the weighted average of all nitrogen fractionation processes occurring in a water column, and the predominance of the nitrogen reactions under specific redox conditions. Lower δ<sup>15</sup>N<sub>bulk</sub> signals are associated with nitrogen fixation in anoxic environments (Beaumont *et al.*, 2000; Galbraith *et al.*, 2008), and nitrification in oxygenated water columns (Altabet and Francois, 1994; Meckler *et al.*, 2007). In contrast, incomplete



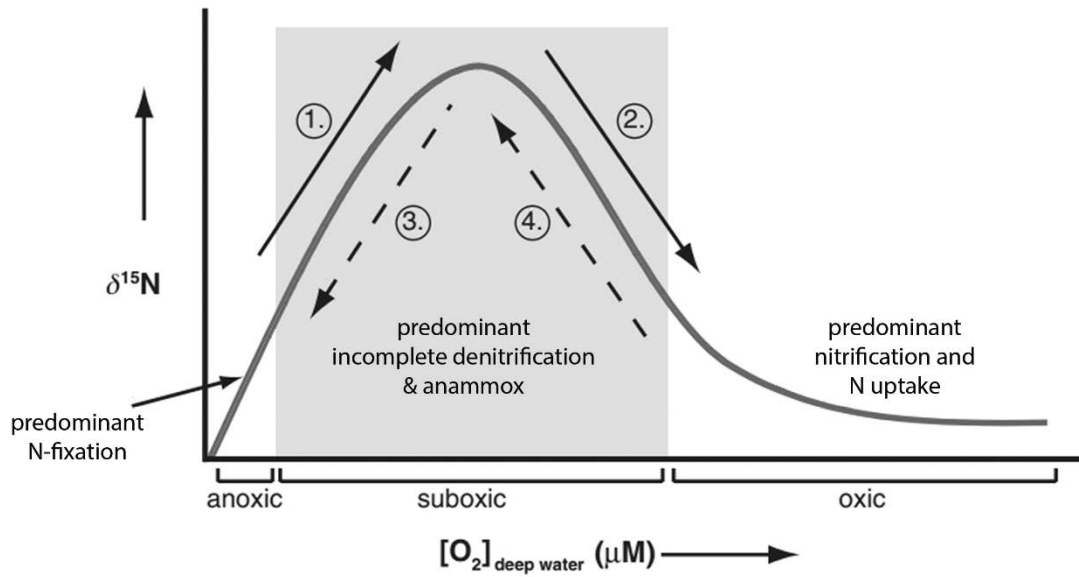


Figure 3. Schematic showing the relationship between bulk sedimentary  $\delta^{15}\text{N}$  values and deep water oxygen concentrations. The relationship between  $\delta^{15}\text{N}$  and oxygen concentrations is nonlinear. Higher  $\delta^{15}\text{N}$  values are associated with denitrification and anammox in suboxic conditions. Lower  $\delta^{15}\text{N}$  values are associated with nitrogen fixation in anoxic conditions and nitrification in oxic environments (Modified from Quan *et al.*, 2013)

denitrification and anammox in suboxic environments result in higher more enriched  $\delta^{15}\text{N}_{\text{bulk}}$  signals (Galbraith *et al.*, 2008; Quan *et al.*, 2008; Brunner *et al.*, 2013). The conceptual model (Fig. 3) can be used to characterize the evolution of oxygen content in a water column at a particular site over time. An increase in  $\delta^{15}\text{N}_{\text{bulk}}$  indicates a transition to a suboxic environment either from anoxic (Arrow 1) or oxic (Arrow 4) conditions, while a shift to lower  $\delta^{15}\text{N}_{\text{bulk}}$  values indicates the transition from suboxia to oxic (Arrow 2) or anoxic conditions (Arrow 3) (Quan *et al.*, 2013).

### 1.2 Diagenetic and catagenetic alterations

Majority of nitrogen isotope analyses have been conducted on samples that have undergone minimal alteration, such as studies constrained to alterations of nitrogen isotopes as particulate OM sinks through the water column (e.g. Altabet and Francois, 1994; Robinson *et al.*, 2012) or diagenesis nearest to the sediment-water interface (e.g.

Müller, 1977; de Lange, 1992; Freudenthal *et al.*, 2001; Lehmann *et al.*, 2002; Möbius *et al.*, 2011). However, subsequent alterations to nitrogen moieties during progressive diagenesis and catagenesis may result in the loss of nitrogen and potentially isotopic fractionation. Alteration of nitrogen is influenced by a variety of factors during diagenesis, including: OM types and concentrations, sedimentation rate, clay content, oxygen concentrations within the upper sediment column, mineralization processes, and aerobic/anaerobic degradation. OM and labile organic nitrogen (ON) can be altered via hydrolysis, carboxylation, fermentation, and deamination processes either by mineralization and biodegradation (Macko, 1981; Macko and Estep, 1984; Rau *et al.*, 1987; Macko *et al.*, 1994; Nguyen and Harvey, 1997; Freudenthal *et al.*, 2001). The macromolecular components (e.g. proteins, carbohydrates, and lipids) of organic detritus are broken down into simpler molecules (e.g. amino acids, sugars, and fatty acids) so they may be used by heterotrophic microbes as a source of metabolism (Killops and Killops, 2005); thereby completing the mineralization of OM. Clay minerals play an important role in the degradation-recondensation of OM by offering protection to amorphous, labile, and simple molecular components from complete microbial degradation (Largeau and Derenne, 1993; Wu *et al.*, 2012 and references therein). The mechanisms responsible remain ambiguous, but it has been hypothesized that preservative mechanisms include: sorption, encapsulation by clay mineral aggregates, and intercalation within expanding clays as organo-mineral nanocomposites (Kennedy *et al.*, 2014 and references therein). Furthermore clays catalytically promote the structural rearrangement of ON into more structurally and thermally stable ON heterocycles and humic complexes; this process is

thought to be similar to natural humification by Maillard reactions and polyphenol theory (Wu *et al.*, 2012 and references therein).

Aqueous  $\text{NH}_4^+$  generation coincides with the onset of oil formation (Hunt, 1979) and illitization of clay minerals (Kennedy, *et al.*, 2014). The coincidence and timing of these three factors is impeccable. During thermal maturation, ON in OM is thermally degraded, and converted to aqueous  $\text{NH}_4^+$  (Williams *et al.*, 1989; Compton *et al.*, 1992; de Lange, 1992; Schroeder and Ingall, 1994; Krooss *et al.*, 1995; Littke *et al.*, 1995; Williams *et al.*, 1995; Freudenthal *et al.*, 2001; Mingram *et al.*, 2003; Jia, 2006; Schimmelmann and Lis, 2010). Ammonium from proteinaceous OM can substitute for  $\text{K}^+$  in adjacent authigenic clays due to the similarities of atomic radii (Williams *et al.*, 1989; Compton *et al.*, 1992; Drits *et al.*, 1997; Papineau *et al.*, 2005). This substitution and illitization causes the clay layers to collapse, which isolates the newly “fixed”  $\text{NH}_4^+$  from further exchange reactions (Williams *et al.*, 1989; Nieder *et al.*, 2011; Kennedy *et al.*, 2104). However, it should be noted that the thermal degradation and generation of  $\text{NH}_4^+$  from OM occurs with isotopic fractionation. Thermal degradation during catagenesis results in the preferential release of light  $^{14}\text{NH}_4^+$  isotope, because it requires less activation energy to cleave  $^{14}\text{N}$  from carbon compared to  $^{15}\text{N}$  (Williams *et al.* 1995; Freudenthal *et al.*, 2001; Mingram and Braüer, 2001; Plessen *et al.*, 2010).

## CHAPTER II

### STUDY AREA

This study focuses on the (Late Devonian) Famennian Ohio Shale of the central Appalachian Basin. The research focuses on analyzing well cutting samples from the A. Lowe Heirs KL4-504695 completed on September 17, 2001 in Pike County, Kentucky (Carter Coordinates: 20-N-84, 2055' FSL, 620' FEL; Latitude: 37.605644, Longitude: -82.50214) (Fig.4). The A. Lowe Heirs KL4-504695 was logged from 0 m (0 ft) to a depth of 1,108 m (3,636 ft). This well proved to be an ideal candidate for this research due to its continuous 209 m (686 ft) section of the Ohio Shale which comprises the lower Huron, middle Huron, upper Huron, Chagrin, and Cleveland equivalent shale members (Fig. 5). The reasoning for defining the uppermost Ohio Shale member as the Cleveland equivalent will be discussed further in more detail shortly.

#### *2.1 Divisions of the Ohio Shale*

The Ohio Shale is the age-equivalent of other Upper Devonian shales such as the New Albany in the Illinois Basin, the Antrim in the Michigan Basin, the Chattanooga in Tennessee, and the Woodford in Oklahoma. Early studies initially divided the Ohio Shale, based on gamma ray signals and total organic carbon content, into the black Huron and Cleveland shale members which were separated by the gray silty-shale Chagrin

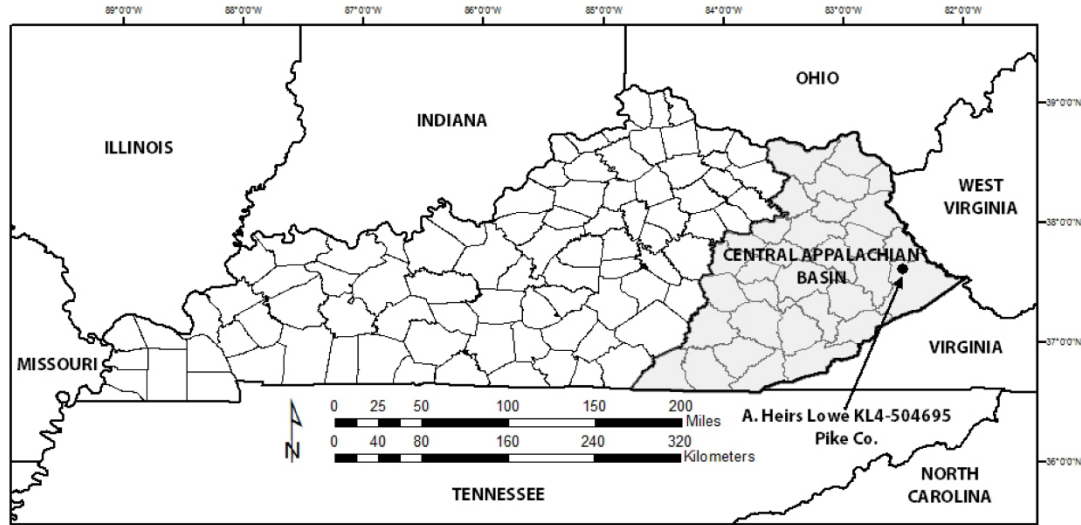


Figure 4. Location of the A. Heirs Lowe KL4-504695 well, Pike Co. (20-N-84, 2055' FSL, 620' FEL) in eastern Kentucky. The extent of the central Appalachian Basin in Kentucky is shown in gray.

Member (Lewis and Schwietering, 1971). Furthermore, the Huron has been subdivided into the lower, middle, and upper Huron members. At our particular study site, the lower Huron Shale is approximately 47 m thick and ranges in colors from very dark gray, brown, very dark brown, to black. Above, the middle Huron Shale is approximately 80 m thick, and varies between predominant gray and dark gray colors with minor pinkish gray intervals. The dark gray to gray upper Huron Member is the thinnest interval at 16 m thick. The 40 m thick Chagrin is the lightest colored member of the Ohio Shale, varying between gray and light gray. The uppermost member of the Ohio Shale is the dark gray Cleveland equivalent, at 26 m thick. Although the Huron and Cleveland members have been described as black shales, based on high gamma ray signals (upwards of 700 API units), TOC content, and color indexing, only the lower Huron Member exhibits black shale qualities. The other members of the Ohio Shale, at our particular location, do not display these qualities; instead, they reflect flych-like clastic sedimentation.

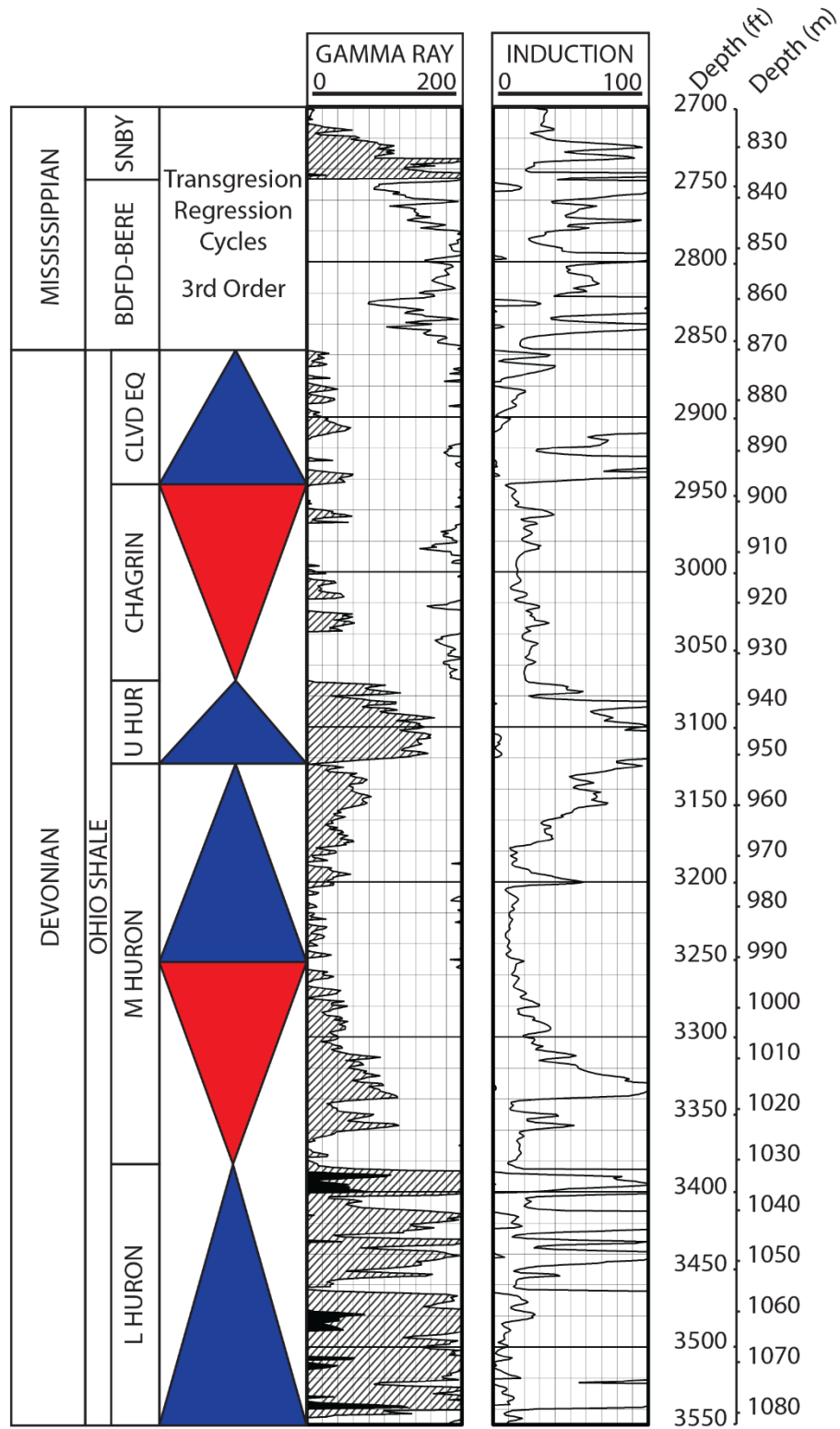
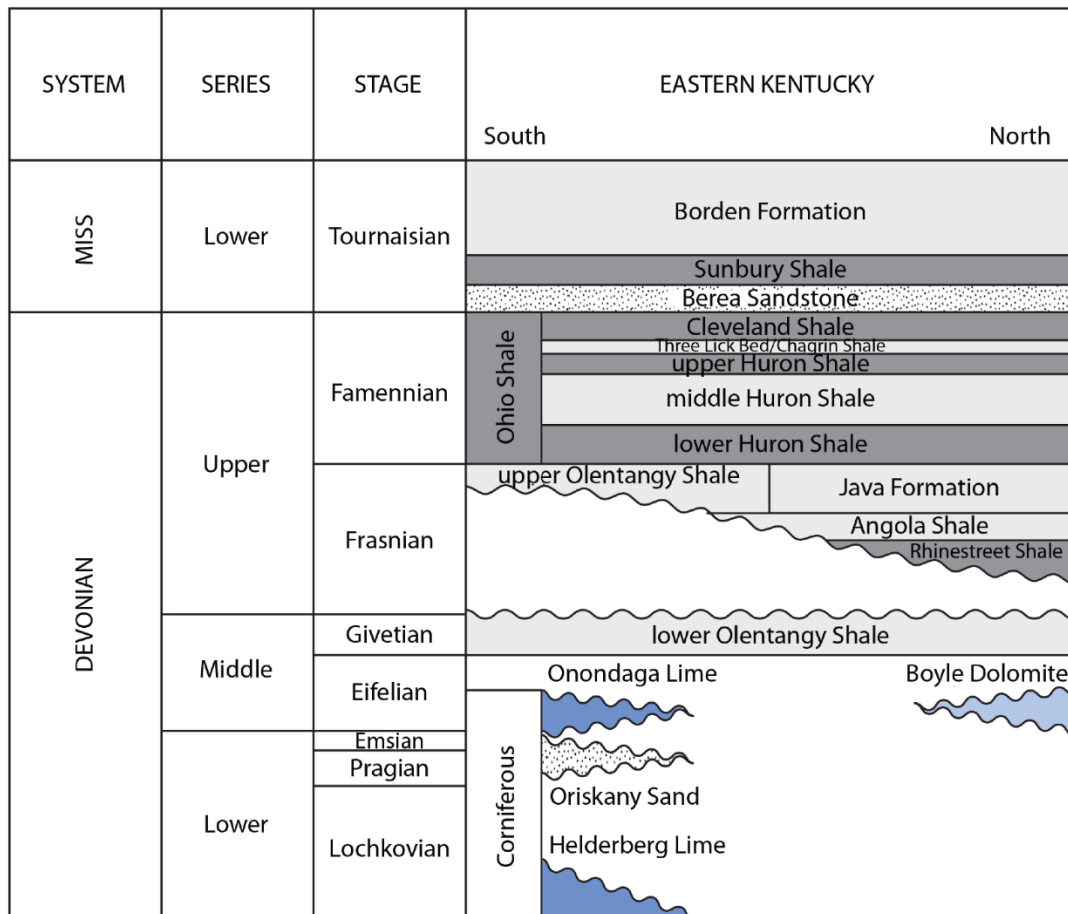


Figure 5. Well log including gamma ray and induction curves for the A. Lowe Heirs KL4-504695 in Pike County, Kentucky. The Ohio Shale includes the following members: lower Huron (L HURON), middle Huron (M HURON), upper Huron (U HUR), Chagrín (CHAGRIN), and Cleveland equivalent (CLVDEQ). Above the Ohio Shale is the Mississippian Bedford-Berea (BDFD-BERE) fluvial sequence and the Sunbury Shale (SNBY)

## 2.2 Stratigraphic framework

In eastern Kentucky, the Famennian Ohio Shale sequence is the stratigraphic interval between the marine Olentangy Shale below, and the fluvial Bedford Formation and the Berea Sandstone above (Fig. 6). The Ohio Shale and its Appalachian Basin equivalents span from western New York, western Pennsylvania, eastern Ohio, through eastern Kentucky, West Virginia, western Virginia, and as far south as Tennessee and Alabama (de Witt, Jr. *et al.*, 1993). Initial studies were able to subdivide the Ohio Shale into black shale and gray shale members via gamma ray log signals, with the latter being characterized by significantly lower gamma ray readings (Lewis and Schwietering, 1971). The Ohio Shale contains includes two predominant sequences of carbonaceous

Figure 6. Generalize stratigraphic column for eastern Kentucky (Modified from Repetski *et al.*, 2013)



black shale, the Huron and Cleveland members, separated by a westward thinning tongue of gray silty-shale of the Chagrin Member (Lewis and Schwietering, 1971; Provo *et al.*, 1978; Neal, 1979; Schwietering, 1979; Hohn *et al.*, 1980; Roen, 1980; Roen, 1984; de Witt, Jr. *et al.*, 1993). Pioneering work by Rich (1951) in the Appalachian Basin was the first to suggest that Late Devonian black shale deposition had a deep-water origin and was so widespread that it can be used as a regional stratigraphic reference.

Early stratigraphic studies of Upper Devonian black shales in the Appalachian and adjacent basins were conducted in a localized fashion (Roen, 1980): leading to the multiple local nomenclatures for similar Devonian shale units within the Appalachian Basin. This prompted various Department of Energy sponsored studies, in order to lay the foundation for a regional stratigraphic correlation between various Upper Devonian shale units within the Appalachian Basin, as well as tying in adjacent basins. Initial stratigraphic correlation studies (e.g. Lewis and Schwietering, 1971; Provo *et al.*, 1978; Neal, 1979; Schwietering, 1979; Hohn *et al.*, 1980; Roen, 1980; Roen, 1984) utilized gamma ray logs from oil and gas wells to lithologically correlate the distribution and extent of shale units throughout the central-eastern United States.

The Huron Member is one of the thickest (upwards of 300 feet), and most prolific hydrocarbon reservoir and extensive black shale unit in the Appalachian Basin, spanning from western New York, through eastern Kentucky, and into Tennessee (Roen, 1984). The Huron is characterized by an anomalously high gamma ray signature, upwards of several hundred API units, making it an ideal candidate for regional stratigraphic correlations. The Huron Member of the Ohio Shale correlates to the lowermost unit in the Gassaway Member of the Chattanooga Shale in southern Kentucky



and Tennessee (Provo *et al.*, 1978; Roen, 1980; Roen, 1984), and the Camp Run Member and majority of the Clegg Creek Member of the New Albany Shale in western Kentucky, Indiana, and Illinois (Robl and Barron, 1988). Much of the regional correlations have focused on the Huron Member as a whole; however, the Huron Member of the Ohio Shale exists as two tongues of black shale separated by the gray middle Huron Shale. To the north, the lower Huron Member is equivalent to the Dunkirk Shale of the Perrysburg Formation in New York (Roen, 1980; de Witt, Jr. *et al.*, 1993). East of Kentucky, the middle Huron Member grades into the lighter colored Brallier gray silty-shale facies in West Virginia (Neal, 1979; Ettensohn *et al.*, 1988). The Chagrin Member, which separates the Huron and Cleveland Members of the Ohio Shale, correlates to the Three Lick Bed in Ohio and north-central Kentucky (Provo *et al.*, 1978; Robl and Barron, 1988), the middle unit of the Gassaway Member of the Chattanooga Shale in southern Kentucky and Tennessee (Roen, 1980; Roen, 1984), and the gray silty-shale and medium siltstones of the Chemung Formation in West Virginia (Neal, 1979). The Cleveland Member of the Ohio Shale correlates to the upper unit of the Gassaway Member in the Chattanooga Shale of Tennessee (Roen, 1980; Roen, 1984), the uppermost Clegg Creek Member of the New Albany Shale in the Illinois Basin (Robl and Barron), and the lower portion of the Big Stone Gap Member in southwestern Virginia (Roen, 1984).

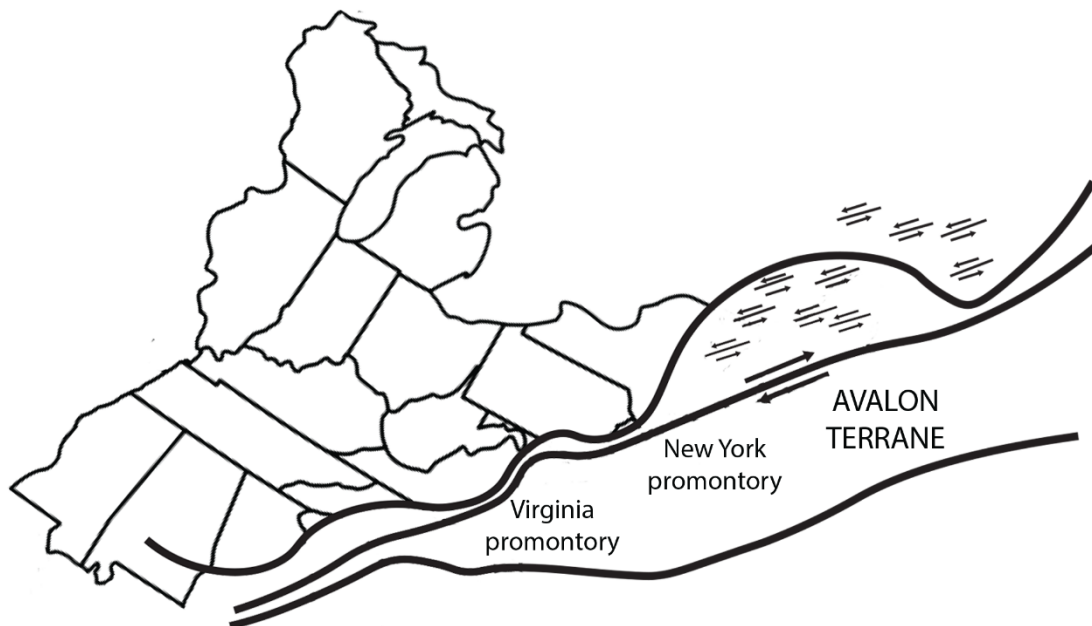
Regional correlations eastward from Kentucky into West Virginia have proven to be difficult for the Cleveland Member. The Cleveland shale was deposited parallel to strike of the paleo-slope of the Appalachian Basin, spanning in a north-south direction from Ohio, through eastern Kentucky, and into Tennessee (Schmoker, 1981; de Witt, Jr. *et al.*, 1993; Pashin and Ettensohn, 1995). Previous studies that conducted isopach

mapping (e.g. Roen, 1980; Roen, 1984) have shown that aerial extent of the Cleveland Shale does not extend into portions of eastern Kentucky, including our study site in Pike County. Gamma ray signals in the Cleveland should be equivalent to those that characterize the Huron Member of the Ohio Shale (Lewis and Schwietering, 1971); however, gamma ray signals for the A. Lowe Heirs KL4-504695 in Pike County show gamma ray values for the Cleveland are similar to those that characterize the Chagrin Member instead of the Huron Member. Schmoker (1981) concluded that the Cleveland Member is about 200 API units below normal in southeastern Kentucky although it is characterized by high TOC contents. The reason for the lack of radioactivity for the Cleveland-equivalent at our study site remains ambiguous. Multiple studies (e.g. Kepferle, 1993; Zheng *et al.*, 2002; Lüning and Kolonic, 2003; Morford *et al.*, 2009) have suggested that the lack of correlation between gamma ray signals and TOC may be due to an array of factors including: high sedimentation rates (dilution), bioturbation and the remobilization of uranium, or irrigation of sediments underlying more oxygenated water columns. Moving eastward from Kentucky, studies have shown that the Cleveland correlates to gray shale and siltstones in West Virginia that are undistinguishable from Chagrin facies; these studies have termed these gray shales above the Huron Members as “undifferentiated” (Neal, 1979; Hohn *et al.*, 1980). Due to the lack of high radioactivity associated with typical Cleveland black shale sequences, the uppermost member of the Ohio Shale at our study site will be defined as the Cleveland equivalent for the remainder of this research.

### 2.3 Acadian Orogeny

The Acadian orogeny (411-315 Ma) was responsible for deposition of Devonian black shales that characterize the Appalachian Basin and other major Paleozoic black shale deposits in North America. The Acadian orogeny was the product of oblique convergence along a large sinistral strike-slip fault zone between the Laurussian and the Avalon terrane (Ettensohn, 1987) (Fig. 7). The Acadian orogeny can be subdivided into four tectocycles, which reflect the successive collisions that migrated southward between different parts of Laurussia and Avalonian fragments (Ettensohn, 1987). The third Acadian tectophase reflects the southward migration of deformation, the collision with the Virginia promontory, and docking of the Carolina terrane: which was responsible for the syn-orogenic deposition of five cycles of black shale sequences (Burket/Genesso, Middlesex, Rhinestreet, Huron, and Cleveland shales) and coarser flysch-like deposits on the western margin of the Appalachian Basin, beginning with the local unconformity of

*Figure 7. Tectonic setting during the Late Devonian Acadian orogeny and the impending collision of the Virginia promontory responsible for the 3rd Acadian tectophase (Modified from Pashin and Ettensohn, 1995)*



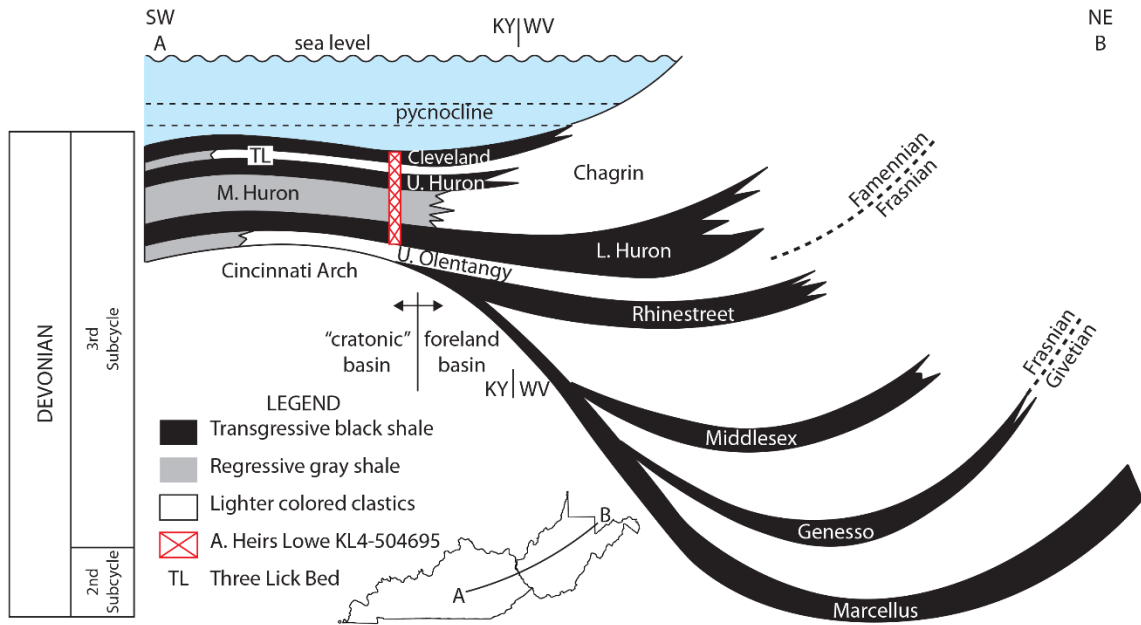


Figure 8. Schematic showing the deposition of black shale, gray shale, and clastic sequences from the Middle to Late Devonian. The yoking of the peripheral bulge (Cincinnati Arch) between the Appalachian and Illinois basins generated the "cratonic" basin, allowing deposition of the Ohio Shale in both basins. Individual formation and member thicknesses are not drawn to scale. (Modified from Ettensohn *et al.*, 1988)

the Taghanic Onlap (Ettensohn, 2008) (Fig 8).

The lithospheric flexural response between the Appalachian and adjacent basins was responsible for the maximum geographic extent of Ohio Shale deposition and its equivalents in the Illinois and Michigan basins. As the fold-thrust belt of the orogen migrates cratonward, the foreland basin and peripheral bulge does as well. Destructive interference between the migrating peripheral bulges of the Illinois and Appalachian basins resulted in the lowering of the arch and yoking of basins (Ettensohn *et al.*, 1988). The yoking of the basins and the lowering of the peripheral bulge (Cincinnati Arch) created a cratonic basin, allowing black shale deposition of the Huron and its equivalents to occur in the Appalachian Basin as well as neighboring basins (Fig. 8). Not until the late Frasnian-early Famennian did the transgressive Rhinestreet and coarser clastic upper Olentangy shales migrate into Kentucky (Ettensohn *et al.*, 1988); however, the lower

Huron and equivalents were the first black shale sequences to extend to multiple basins. The infilling of the foreland basin and the cratonward shift of black shale facies records the vast extent and advancement of Acadian deformation, as well as the transgression of black shale subcycles during the third tectophase (Ettensohn, 1987; Ettensohn, 1992; Ettensohn, 2008). It was suggested by Ettensohn *et al.* (1988) that the merging of the Appalachian, Illinois, and Michigan basins acted like intracratonic depressions within a single larger basin, due to the excessive flysch-like clastic influx.

#### 2.4 Eustasy

Tectonism alone has the ability to affect subsidence and the progradation of black shales sequences in a foreland basin (e.g. Ettensohn, 2008), but early depositional models (e.g. Ettensohn and Barron, 1981) suggested that lateral transition from transgressive black shale facies to regressive gray shales was governed by eustasy, and the vertical movement of the pycnocline during times of increased plate convergence or times of tectonic quiescence. Early depositional models advocated that transgressive and regressive shales were structurally controlled. However, by the Famennian the third Acadian tectophase was waning and the deformational front was far from the locus of convergence that subsidence was overwhelmed by increasing flysch-like clastic influx (Ettensohn *et al.*, 1988). Although tectonism, or the lack thereof may have an influence on the cyclicity of sequential transgressive and regressive shale facies, other eustatic factors should be incorporated in order to fully understand the various transgressive and regressive sequences within formations and between individual members.

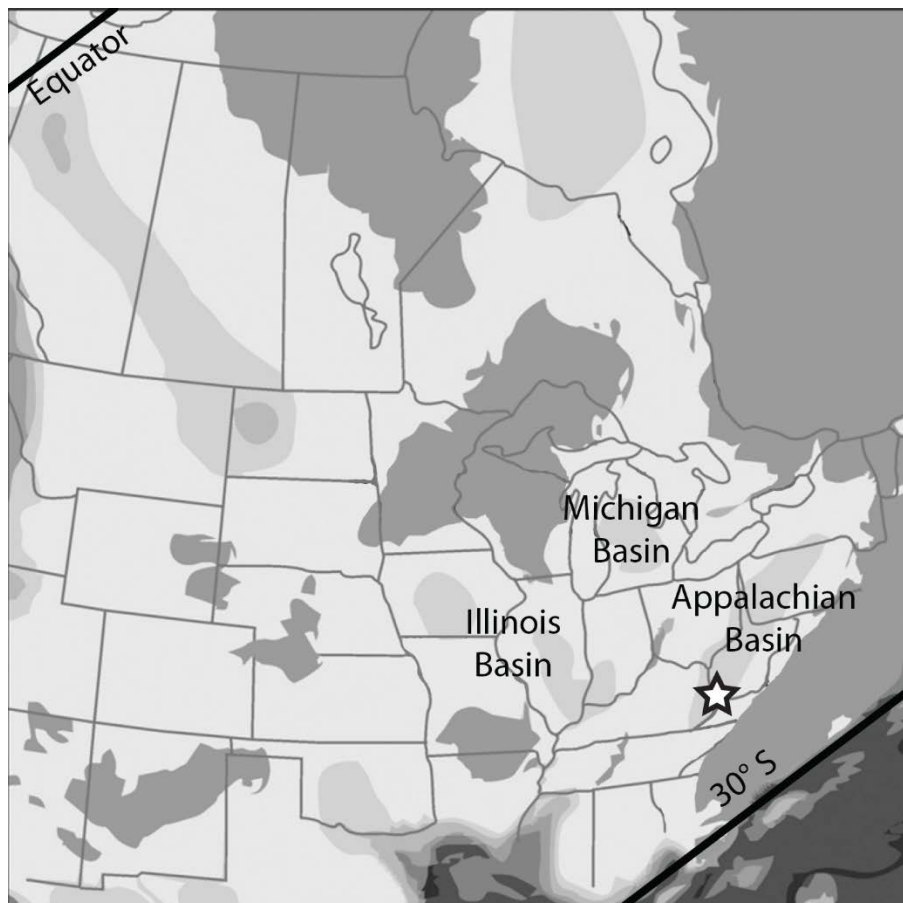
Johnson *et al.* (1985) was one of the first to evaluate shelf sedimentary facies transitions from around the world in attempts to produce a more reliable paradigm for Devonian eustatic sea-level fluctuations. They concluded that early Famennian initiated with eustatic deepening, and the deposition of the transgressive lower Huron equivalent Dunkirk Shale. Following this initial transgression, the Famennian was characterized by prominent regressive tendencies (Johnson *et al.*, 1985; Haq and Schutter, 2008), leading to the lowstand deposition and reworking of the Bedford-Berea Delta complex during the latest Famennian (Ettensohn, 2008). The mechanism(s) responsible for the overall regressive tendencies seen in the Famennian have led to multiple hypotheses. After evaluating depositional sequences of Upper Devonian Catskill Delta margin sedimentation, Tassell (1987) proposed that deposition of sedimentary sequences in the Acadian third tectophase were strongly influenced astronomically controlled 100,000 year cycles related to the orbital eccentricity of Earth, as well as smaller scale 40,000 and 20,000 year cycles related to precession and tilt orbital variations. Subsequent studies have proposed the forcing mechanisms for Famennian regression include glacial-eustatic (e.g. Pashin and Ettensohn, 1995; Filer, 2002; Ettensohn, 2008; Haq and Schutter, 2008; Isaacson *et al.*, 2008; McClung *et al.*, 2013). Late Devonian glacial deposits in the form of tillites have been well documented in Brazil, Bolivia and other Andean provinces in South America (Isaacson *et al.*, 2008). Coeval evidence for Alpine glaciation in the Appalachians, have been identified in the form of diamictities (Brezinksi *et al.*, 2008; Brezinksi *et al.*, 2009). The paleoclimatic transition from greenhouse to more icehouse conditions during the Late Devonian led to Famennian glaciation and the overall eustatic regression (Ettensohn, 2008; McClung *et al.*, 2013). Eustatic drawdown during the

Famennian glaciation, along with increased tectonism during the third Acadian tectocycle, resulted in the progradation of black shale and flysch-like clastics wedges cratonward in the Appalachian Basin. Shorter-term changes in Famennian sea-level may have been a result of third order eustatic cycles sequences (upwards of a few million years).

### 2.5 Controls of organic carbon in the central Appalachian Basin

Paleogeographic reconstructions of North America (Fig. 9) shows that black shale deposition occurred in a large, nearly enclosed embayment in a tradewind belt near the northern margin of the temperate zone (Ettensohn, 2008). Various studies (e.g. Ettensohn

*Figure 9. Late Devonian paleogeographic map of North America showing the Appalachian Basin. Sample location of the A. Lowe Heirs KL4-504695 is designated by the white star (Modified from Formolo et al., 2014)*



and Barron, 1981; Ettensohn *et al.*, 1988; Robl and Barron; 1988; Pashin and Ettensohn, 1992; Ingall *et al.*, 1993; Kepferle, 1993; Murphy *et al.*, 2000; Werne *et al.*, 2002; Sageman *et al.*, 2003; Rimmer, 2004, Rimmer *et al.*, 2004; Perkins *et al.*, 2008) have proposed multiple explanations for Ohio Shale and other Upper Devonian shale deposition, including: paleoredox conditions and the location of the pycnocline with respect to the site of deposition, dilution and sediment starvation, decomposition rates of organic matter (OM), rates of primary production, nutrient fluxes, coupled feedback mechanisms, and other environmental and hydrodynamic factors. Geochemical, petrographical, and faunal distribution analyses conducted by these studies concluded that organic rich shale deposition is not regulated by one single controlling factor, but controlled by a variety of elements. While it is hard to constrain all of the before mentioned factors, bulk nitrogen isotopes with other geochemical proxies can be used to evaluate the paleoredox conditions and the evolution of Ohio Shale deposition, and the controls of organic carbon preservation in eastern Kentucky.



## CHAPTER III

### METHODOLOGY

Well cuttings from the A. Lowe Heirs KL4-504695 were collected at approximately 3 m intervals from the Kentucky Geological Survey well sample and core library in Lexington, Kentucky. The approximate range of sample spacing is associated with the drilling and mud logging processes. Mud loggers have to account for the lag time for well cuttings to be brought up hole and to the surface where they are caught. Three meter intervals allow best averages for well cutting sample depth calibration with minimal error. However, inaccuracies in sample depth calibration, due to caving and sample contamination during the drilling process, may occur. The validity of our data will be discussed in further detail later. Once samples were selected, shale chips were transported to the Noble Research Center at Oklahoma State University for sample preparation. Shale chips were then crushed and ground into a fine powder using an agate mortar and pestle. The crushed samples were then oven-dried for approximately 24 hours at 60°C in order to remove any residual water, and stored in glass vials.

#### *3.1 Stable isotopic compositions and elemental concentrations*

Powdered samples were analyzed for bulk nitrogen ( $\delta^{15}\text{N}_{\text{bulk}}$ ), inorganic nitrogen ( $\delta^{15}\text{N}_{\text{inorg}}$ ), and organic carbon ( $\delta^{13}\text{C}_{\text{org}}$ ) isotopic values, and total nitrogen (TN),

inorganic nitrogen (IN), and total organic carbon (TOC) bulk elemental concentrations. The analyses were conducted in the geochemistry laboratory at the Henry Bellman Research Center at Oklahoma State University. Bulk and inorganic nitrogen and organic carbon delta values ( $\delta^{15}\text{N}_{\text{bulk}}$ ,  $\delta^{15}\text{N}_{\text{inorg}}$ , and  $\delta^{13}\text{C}_{\text{org}}$ ) and elemental concentrations (TOC, TN, IN) were determined using a Costech ECS 4010 elemental analyzer (EA) coupled with a ThermoFinnigan Deltaplus XL isotope ratio mass spectrometer (IRMS). The isotopic values are reported relative to air  $\text{N}_2$  standard for bulk and inorganic nitrogen ratios, and Vienna Pee Dee Belemnite (VPDB) standard for organic carbon ratios. The isotopic compositions are expressed in delta ( $\delta$ ) notation in parts per mil (‰):

$$\delta(\text{‰}) = \left[ \frac{R_{\text{sample}}}{R_{\text{standard}}} - 1 \right] \times 1000 \quad (\text{Eq. 3.1: delta notation})$$

where  $R_{\text{sample}} = {}^{13}\text{C}/{}^{12}\text{C}_{\text{sample}}$  OR  ${}^{15}\text{N}/{}^{14}\text{N}_{\text{sample}}$  and  $R_{\text{standard}} = {}^{13}\text{C}/{}^{12}\text{C}_{\text{VPDB}}$   ${}^{15}\text{N}/{}^{14}\text{N}_{\text{air}}$ .

Raw data were calibrated using standards of known isotopic composition to correct for any isotopic offset. NIST N3 ( $\text{KNO}_3$ ) and USGS 40 (L-glutamic acid) standards were used for nitrogen isotopic calibrations, while urea ( $\text{CH}_4\text{N}_2\text{O}$ ) and USGS 40 were used for carbon isotopes and TOC concentrations. An acetanilide ( $\text{C}_8\text{H}_9\text{NO}$ ) standard was used to check for machine drift and calibrate elemental concentrations during each sample run. Replicates of nitrogen standards USGS 40 and  $\text{KNO}_3$  had a standard deviation of  $\pm 0.2\text{‰}$  and  $\pm 0.1\text{‰}$ , respectively. Replicates of the  $\delta^{15}\text{N}_{\text{bulk}}$  and  $\delta^{15}\text{N}_{\text{inorg}}$  samples for the A. Lowe Heirs KL4-504695 had standard deviations of  $\pm 0.2\text{‰}$  and  $\pm 0.3\text{‰}$ , respectively. Replicates of carbon standards USGS 40 and urea had a standard deviation of  $\pm 0.2\text{‰}$  and  $\pm 0.3\text{‰}$ , and replicate samples for  $\delta^{13}\text{C}_{\text{org}}$  had a standard deviation of  $\pm 0.3\text{‰}$ . For individual sample runs, 3 samples were run as

duplicates and 1 as a triplicate, with standards every 10 samples in order to ensure precision and reproducibility.

### 3.2 Laboratory procedures

To analyze for TN and  $\delta^{15}\text{N}_{\text{bulk}}$ , approximately 35 mg of each powdered sample was placed into an individual tin boat. A vanadium pentoxide catalyst was added to each sample to help ensure complete combustion during analyses. In order to evaluate for IN and  $\delta^{15}\text{N}_{\text{inorg}}$ , cutting samples had to undergo additional preparation before analyses. This required ON to be removed from samples using a potassium hypobromite (KOBr) digestion method as described by Silva and Bremner (1966). Inorganic nitrogen in the form of fixed and exchangeable ammonium is typically determined using the Kjeldahl distillation method as described by Bremner and Keeney (1966); however this method involves tedious and difficult digestion, distillation, and titration steps. In a study by Minagawa *et al.* (1984), the Kjeldahl digestion and distillation method of complex OM did not provide complete chemical yields when evaluating for separate nitrogen species isotopic values compared to the KOBr digestion and combustion method described below. By definition, exchangeable nitrogen is the  $\text{NH}_4^+$  that is extractable by a 2 M KCl solution, while fixed ammonium is the fraction that is not by 2 M KCl, but liberated after being subjected to a hypobromite solution (de Lang, 1992; Freudenthal *et al.*, 2001). Therefore, for the remainder of this research, IN will refer to  $\text{NH}_4^+$  fixed within clay minerals. Since this method utilizes liquid bromine, extreme caution is advised.

The exact digestion method used by Tuite Jr. (2012) is as follows. The KOBr-KOH solution was prepared by adding 6 ml of bromine at 0.5 ml/minute to 200 ml of 2

M KOH while cooling the solution in an ice bath. Twenty ml of prepared KOB<sub>r</sub>-KOH solution was added to a flask containing 500-1000 mg of powdered sample, swirled, and left for 2 hours. 60 ml of deionized (DIW) was added to the flask and the contents were brought to a boil for 10 minutes on a hot plate then allowed to cool overnight. The supernatant fluid was removed and the samples were washed in 0.5 M KCl. Samples were then washed in de-ionized water (DIW) water until pH of the supernatant achieved neutrality, and then dried at approximately 50°C overnight. Analyses for inorganic nitrogen isotope measurements then followed the same procedure as bulk nitrogen samples.

To analyze for TOC and  $\delta^{13}\text{C}_{\text{org}}$ , approximately 10 mg of sample was progressively decarbonated in silver boats. Samples were first decarbonated using 25% HCl, then concentrated HCl until effervescence ceased. Once the decarbonation process was complete samples were dried at approximately 60°C for 3 days in order to ensure complete dryness and wrapped in tin capsules. Following drying the samples, the same procedure described for TN and  $\delta^{15}\text{N}_{\text{bulk}}$  were carried out.

### *3.3 Calibration, quality control, and statistical analysis*

Calibration of  $\delta$ -values for a particular set of samples is determined by using isotopic standards. Primary standards ( $\text{N}_2$  air for nitrogen and VPDB for carbon) have a definitive  $\delta$ -value, and are crucial for the standardization of isotopic measurements. This enables the comparison of data sets between multiple laboratories. Secondary standards (NIST N3, USGS 40, and Urea) are natural and synthetic compounds that have been calibrated to primary standards and the  $\delta$ -values of these materials are agreed upon

internationally (Carter and Barwick, 2011). The raw  $\delta$ -values of these secondary standards are then averaged, and the difference between the averaged raw  $\delta$ -value and the actual secondary standard data is used to adjust raw  $\delta$ -values for the sediment/gas/liquid samples: this process is referred to as normalization. If raw secondary standard  $\delta$ -values have a large standard deviation, then adjusted sample  $\delta$ -values will be less precise and be subjected to greater uncertainty. This is because secondary standards should display linearity, which refers to the ability of the measurement procedure to produce  $\delta$ -values that are independent of the amount of material analyzed (Carter and Barwick, 2011). Likewise, if a progressive trend in raw standard  $\delta$ -values is observed (e.g.  $\delta$ -values are constantly decreasing or increasing during the sample run), machine drift may likely be occurring. To confirm machine drift, acetanilide standards are run to monitor the hourly and daily performance of an IRMS. Drift arises when an instrument response changes over time, which is often associated with changes in ambient temperature or the stability of electric circuits; however, machine drift can be properly corrected using specific algorithms (Cheatham *et al.*, 1993). Duplicate and triplicate replicate samples should also be included during each IRMS sample run in order to check for reproducibility. The standard deviation of these duplicate and triplicate samples should have a target standard deviation equal to or less than 0.3 ‰ for nitrogen and carbon isotopic analyses (Carter and Barwick, 2011). Standard deviation values larger than this threshold lead to greater uncertainties when adjusting and correcting for true sample  $\delta$ -values. Statistical analyses for reproducibility of sample and standard  $\delta$ -values have proven mass spectrometry analyses conducted in this research are within the accepted quality assurance threshold. Minimum, maximum, average, and standard deviations of geochemical results for

individual members are presented for the lower Huron (Table 1), middle Huron (Table 2), upper Huron (Table 3), Chagrin (Table 4), and Cleveland equivalent (Table 5) shales.

## CHAPTER IV

### RESULTS

Results of isotopic and elemental concentrations for  $\delta^{15}\text{N}_{\text{bulk}}$  (‰),  $\delta^{15}\text{N}_{\text{inorganic}}$  (‰), TN (wt. %), IN (wt. %),  $\delta^{13}\text{C}_{\text{org}}$  (‰), TOC (wt. %), and  $\text{C}_{\text{org}}/\text{TN}$  are presented in Appendix I, and plotted with respect to depth in Figure 10.

#### 4.1 Geochemical results: lower Huron Member

Sedimentary  $\delta^{15}\text{N}_{\text{bulk}}$  values range from -1.2 to -2.5‰ with a mean  $\delta^{15}\text{N}_{\text{bulk}}$  value of  $-1.8 \pm 0.4$ ‰. Sedimentary  $\delta^{15}\text{N}_{\text{inorg}}$  values vary from -1.5 to -2.1‰ with a mean  $\delta^{15}\text{N}_{\text{inorganic}}$  value of  $-1.7 \pm 0.2$ ‰. Total nitrogen varies from 1.6 to 1.9 wt. % and has a mean value of  $1.7 \pm 0.1$ %; IN concentrations range from 1.3 to 1.7 wt. % with a mean value of  $1.5 \pm 0.1$ %. Maximum and minimum  $\delta^{13}\text{C}_{\text{org}}$  values range from -29.1 to -30.6‰ with a mean isotopic value of  $-30.1 \pm 0.4$ ‰. TOC values vary from 3.8 to 9.3 wt. % with a mean concentration of  $5.7 \pm 1.4$  wt. %.

Table 1. Minimum, maximum, average, and standard deviation values for  $\delta^{15}\text{N}_{\text{bulk}}$  (‰),  $\delta^{15}\text{N}_{\text{inorg}}$  (‰), TN (wt. %), IN (wt. %),  $\delta^{13}\text{C}_{\text{org}}$  (‰), TOC (wt. %), and  $\text{C}_{\text{org}}/\text{TN}$  values the lower Huron Member.

LOWER HURON MEMBER							
	$\delta^{15}\text{N}_{\text{bulk}}$ (‰)	$\delta^{15}\text{N}_{\text{inorg}}$ (‰)	TN (wt %)	IN (wt %)	$\delta^{13}\text{C}_{\text{org}}$ (‰)	TOC (wt %)	$\text{C}_{\text{org}}/\text{TN}$
MIN	-2.5	-2.1	1.6	1.3	-30.6	3.8	2.4
MAX	-1.2	-1.5	1.9	1.7	-29.1	9.3	5.4
MEAN	-1.8	-1.7	1.7	1.5	-30.1	5.7	3.3
STD DEV	0.4	0.2	0.1	0.1	0.4	1.4	0.8

#### 4.2 Geochemical results: middle Huron Member

Sedimentary  $\delta^{15}\text{N}_{\text{bulk}}$  values range from -0.2 to -2.3‰ with a mean  $\delta^{15}\text{N}_{\text{bulk}}$  value of  $-1.1 \pm 0.5\text{‰}$ . Sedimentary  $\delta^{15}\text{N}_{\text{inorg}}$  values vary from -0.7 to -1.6‰ with a mean  $\delta^{15}\text{N}_{\text{inorganic}}$  value of  $-1.0 \pm 0.2\text{‰}$ . Total nitrogen varies from 1.1 to 1.6 wt. % and has a mean value of  $1.4 \pm 0.1\%$ ; IN concentrations range from 0.9 to 1.4 wt. % with a mean value of  $1.2 \pm 0.1\%$ . Maximum and minimum  $\delta^{13}\text{C}_{\text{org}}$  values range from -25.2 to -29.7‰ with a mean isotopic value of  $-27.5 \pm 1.4\text{‰}$ . TOC values vary from 0.5 to 4.4 wt. % with a mean concentration of  $1.5 \pm 1.2$  wt. %.

Table 2. Minimum, maximum, average, and standard deviation values for  $\delta^{15}\text{N}_{\text{bulk}}$  (‰),  $\delta^{15}\text{N}_{\text{inorg}}$  (‰), TN (wt. %), IN (wt. %),  $\delta^{13}\text{C}_{\text{org}}$  (‰), TOC (wt. %), and  $C_{\text{org}}/\text{TN}$  values the middle Huron Member.

MIDDLE HURON MEMBER							
	$\delta^{15}\text{N}_{\text{bulk}}$ (‰)	$\delta^{15}\text{N}_{\text{inorg}}$ (‰)	TN (wt %)	IN (wt %)	$\delta^{13}\text{C}_{\text{org}}$ (‰)	TOC (wt %)	$C_{\text{org}}/\text{TN}$
<b>MIN</b>	-2.3	-1.6	1.1	0.9	-29.7	0.5	0.4
<b>MAX</b>	-0.2	-0.7	1.6	1.4	-25.2	4.4	2.8
<b>MEAN</b>	-1.1	-1.0	1.4	1.2	-27.5	1.5	1.1
<b>STD DEV</b>	0.5	0.2	0.1	0.1	1.4	1.2	0.8

#### 4.3 Geochemical results: upper Huron Member

Sedimentary  $\delta^{15}\text{N}_{\text{bulk}}$  values range from -1.1 to -1.9‰ with a mean  $\delta^{15}\text{N}_{\text{bulk}}$  value of  $-1.4 \pm 0.3\text{‰}$ . Sedimentary  $\delta^{15}\text{N}_{\text{inorg}}$  values vary from -0.8 to -1.1‰ with a mean  $\delta^{15}\text{N}_{\text{inorganic}}$  value of  $-1.0 \pm 0.1\text{‰}$ . Total nitrogen varies from 1.5 to 1.7 wt. % and has a mean value of  $1.6 \pm 0.1\%$ ; IN concentrations range from 1.2 to 1.3 wt. % with a mean value of  $1.3 \pm 0.1\%$ . Maximum and minimum  $\delta^{13}\text{C}_{\text{org}}$  values range from -27.6 to -28.7‰ with a mean isotopic value of  $-28.2 \pm 0.5\text{‰}$ . TOC values vary from 2.6 to 3.8 wt. % with a mean concentration of  $3.1 \pm 0.6$  wt. %.



Table 3. Minimum, maximum, average, and standard deviation values for  $\delta^{15}\text{N}_{\text{bulk}}$  (‰),  $\delta^{15}\text{N}_{\text{inorg}}$  (‰), TN (wt. %), IN (wt. %),  $\delta^{13}\text{C}_{\text{org}}$  (‰), TOC (wt. %), and  $C_{\text{org}}/\text{TN}$  values the upper Huron Member.

UPPER HURON MEMBER							
	$\delta^{15}\text{N}_{\text{bulk}}$ (‰)	$\delta^{15}\text{N}_{\text{inorg}}$ (‰)	TN (wt %)	IN (wt %)	$\delta^{13}\text{C}_{\text{org}}$ (‰)	TOC (wt %)	$C_{\text{org}}/\text{TN}$
<b>MIN</b>	-1.9	-1.1	1.5	1.2	-28.7	2.6	1.7
<b>MAX</b>	-1.1	-0.8	1.7	1.3	-27.6	3.8	2.4
<b>MEAN</b>	-1.4	-1.0	1.6	1.3	-28.2	3.1	2.0
<b>STD DEV</b>	0.3	0.1	0.1	0.1	0.5	0.6	0.3

#### 4.4 Geochemical results: Chagrin Member

Sedimentary  $\delta^{15}\text{N}_{\text{bulk}}$  values range from -1.9 to 0.8‰ with a mean  $\delta^{15}\text{N}_{\text{bulk}}$  value of  $-0.1 \pm 0.6\text{‰}$ . Sedimentary  $\delta^{15}\text{N}_{\text{inorg}}$  values vary from -0.6 to 0.0‰ with a mean  $\delta^{15}\text{N}_{\text{inorganic}}$  value of  $-0.3 \pm 0.2\text{‰}$ . Total nitrogen varies from 0.9 to 1.4 wt. % and has a mean value of  $1.0 \pm 0.2\%$ : IN concentrations range from 0.7 to 1.1 wt. % with a mean value of  $0.9 \pm 0.1\%$ . Maximum and minimum  $\delta^{13}\text{C}_{\text{org}}$  values range from -24.8 to -28.5‰ with a mean isotopic value of  $-26.3 \pm 0.3\text{‰}$ . TOC values vary from 0.3 to 2.1 wt. % with a mean concentration of  $0.8 \pm 0.6$  wt. %.

Table 4. Minimum, maximum, average, and standard deviation values for  $\delta^{15}\text{N}_{\text{bulk}}$  (‰),  $\delta^{15}\text{N}_{\text{inorg}}$  (‰), TN (wt. %), IN (wt. %),  $\delta^{13}\text{C}_{\text{org}}$  (‰), TOC (wt. %), and  $C_{\text{org}}/\text{TN}$  values the Chagrin Member.

CHAGRIN MEMBER							
	$\delta^{15}\text{N}_{\text{bulk}}$ (‰)	$\delta^{15}\text{N}_{\text{inorg}}$ (‰)	TN (wt %)	IN (wt %)	$\delta^{13}\text{C}_{\text{org}}$ (‰)	TOC (wt %)	$C_{\text{org}}/\text{TN}$
<b>MIN</b>	-1.9	-0.6	0.9	0.7	-28.5	0.3	0.3
<b>MAX</b>	0.8	0.0	1.4	1.1	-24.8	2.1	1.7
<b>MEAN</b>	-0.1	-0.3	1.0	0.9	-26.3	0.8	0.7
<b>STD DEV</b>	0.6	0.2	0.2	0.1	1.3	0.6	0.5

#### 4.5 Geochemical results: Cleveland equivalent Member

Sedimentary  $\delta^{15}\text{N}_{\text{bulk}}$  values range from -0.5 to 1.6‰ with a mean  $\delta^{15}\text{N}_{\text{bulk}}$  value of  $1.1 \pm 0.4\text{‰}$ . Sedimentary  $\delta^{15}\text{N}_{\text{inorg}}$  values vary from 0.5 to 1.6‰ with a mean  $\delta^{15}\text{N}_{\text{inorganic}}$

value of  $1.0 \pm 0.4\%$ . Total nitrogen varies from 1.2 to 1.9 wt. % and has a mean value of  $1.5 \pm 0.2\%$ : IN concentrations range from 1.0 to 1.7 wt. % with a mean value of  $1.2 \pm 0.2\%$ . Maximum and minimum  $\delta^{13}\text{C}_{\text{org}}$  values range from -28.2 to -29.0‰ with a mean isotopic value of  $-28.7 \pm 0.3\%$ . TOC values vary from 4.1 to 9.4 wt. % with a mean concentration of  $6.1 \pm 1.7$  wt. %.

*Table 5. Minimum, maximum, average, and standard deviation values for  $\delta^{15}\text{N}_{\text{bulk}}$  (‰),  $\delta^{15}\text{N}_{\text{inorg}}$  (‰), TN (wt. %), IN (wt. %),  $\delta^{13}\text{C}_{\text{org}}$  (‰), TOC (wt. %), and  $\text{C}_{\text{org}}/\text{TN}$  values the Cleveland equivalent.*

CLEVELAND EQUIVALENT MEMBER							
	$\delta^{15}\text{N}_{\text{bulk}}$ (‰)	$\delta^{15}\text{N}_{\text{inorg}}$ (‰)	TN (wt %)	IN (wt %)	$\delta^{13}\text{C}_{\text{org}}$ (‰)	TOC (wt %)	$\text{C}_{\text{org}}/\text{TN}$
<b>MIN</b>	0.5	0.5	1.2	1.0	-29.0	4.1	3.3
<b>MAX</b>	1.6	1.6	1.9	1.7	-28.2	9.4	4.9
<b>MEAN</b>	1.1	1.0	1.5	1.2	-28.7	6.1	4.0
<b>STD DEV</b>	0.4	0.4	0.2	0.2	0.3	1.7	0.7

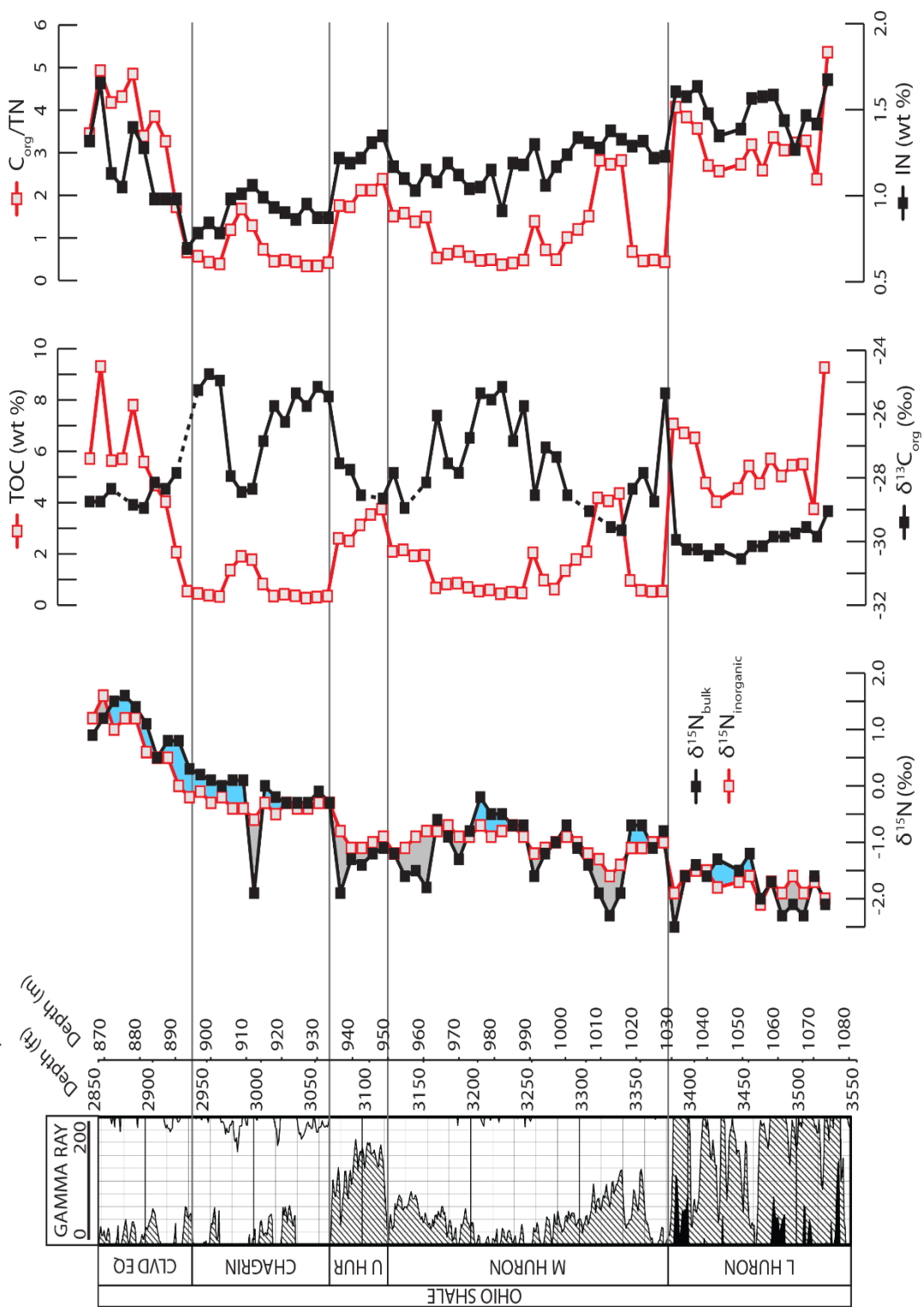


Figure 10. Bulk nitrogen isotope ( $\delta^{15}\text{N}_{\text{bulk}}$ ), inorganic nitrogen isotope ( $\delta^{15}\text{N}_{\text{inorganic}}$ ), organic carbon isotope ( $\delta^{13}\text{C}_{\text{org}}$ ), total organic carbon (TOC), inorganic nitrogen (IN), and  $C_{\text{org}}/\text{TN}$  profiles for the individual members of the Ohio Shale: lower Huron, middle Huron, upper Huron, Chagrin, and Cleveland equivalent. Values are relative to the gamma ray log for the A. Lowe Heirs KL4-504695 well in Pike Co., KY. Positive crossover ( $\delta^{15}\text{N}_{\text{bulk}} > \delta^{15}\text{N}_{\text{inorganic}}$ ) are shaded blue, negative crossovers ( $\delta^{15}\text{N}_{\text{bulk}} < \delta^{15}\text{N}_{\text{inorganic}}$ ) are shaded gray.

## CHAPTER V

### DISCUSSION

#### *5.1 Paleoredox evolution and depositional model of the Ohio Shale*

Using  $\delta^{15}\text{N}_{\text{bulk}}$  and TOC as our proxies for oxygen content and preservation of OM, it is possible to evaluate the paleoredox evolution (Fig. 11) and build a depositional model for our particular site in eastern Kentucky (Fig. 12). Anoxic conditions would promote nitrogen fixation as the predominant biogeochemical process that leads to low sedimentary  $\delta^{15}\text{N}_{\text{bulk}}$  values, and greater quantities of preserved OM. In contrast, suboxic water column conditions would lead to minimal OM preservation and promote denitrification as the predominant reaction resulting in higher sedimentary  $\delta^{15}\text{N}_{\text{bulk}}$  values.

The lower Huron Member was deposited in an anoxic system below the pycnocline, as indicated by low  $\delta^{15}\text{N}_{\text{bulk}}$  values and high TOC. The middle Huron was deposited in alternating suboxic and anoxic conditions, suggesting deposition at our particular site fluctuated within the pycnocline and below it. This is confirmed by the large ranges and standard deviations of  $\delta^{15}\text{N}_{\text{bulk}}$  and TOC values. The upper Huron was deposited below the pycnocline in anoxic conditions: indicated by lower  $\delta^{15}\text{N}_{\text{bulk}}$  and high TOC contents. The Chagrin Member was predominantly deposited in a suboxic environment within the pycnocline as characterized by higher  $\delta^{15}\text{N}_{\text{bulk}}$  and high TOC.

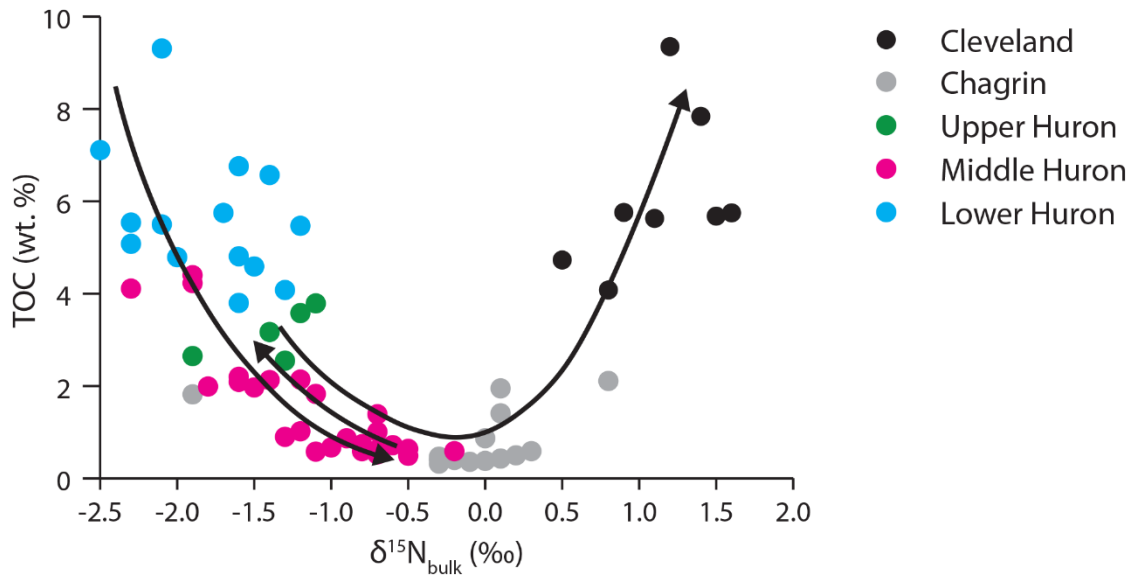
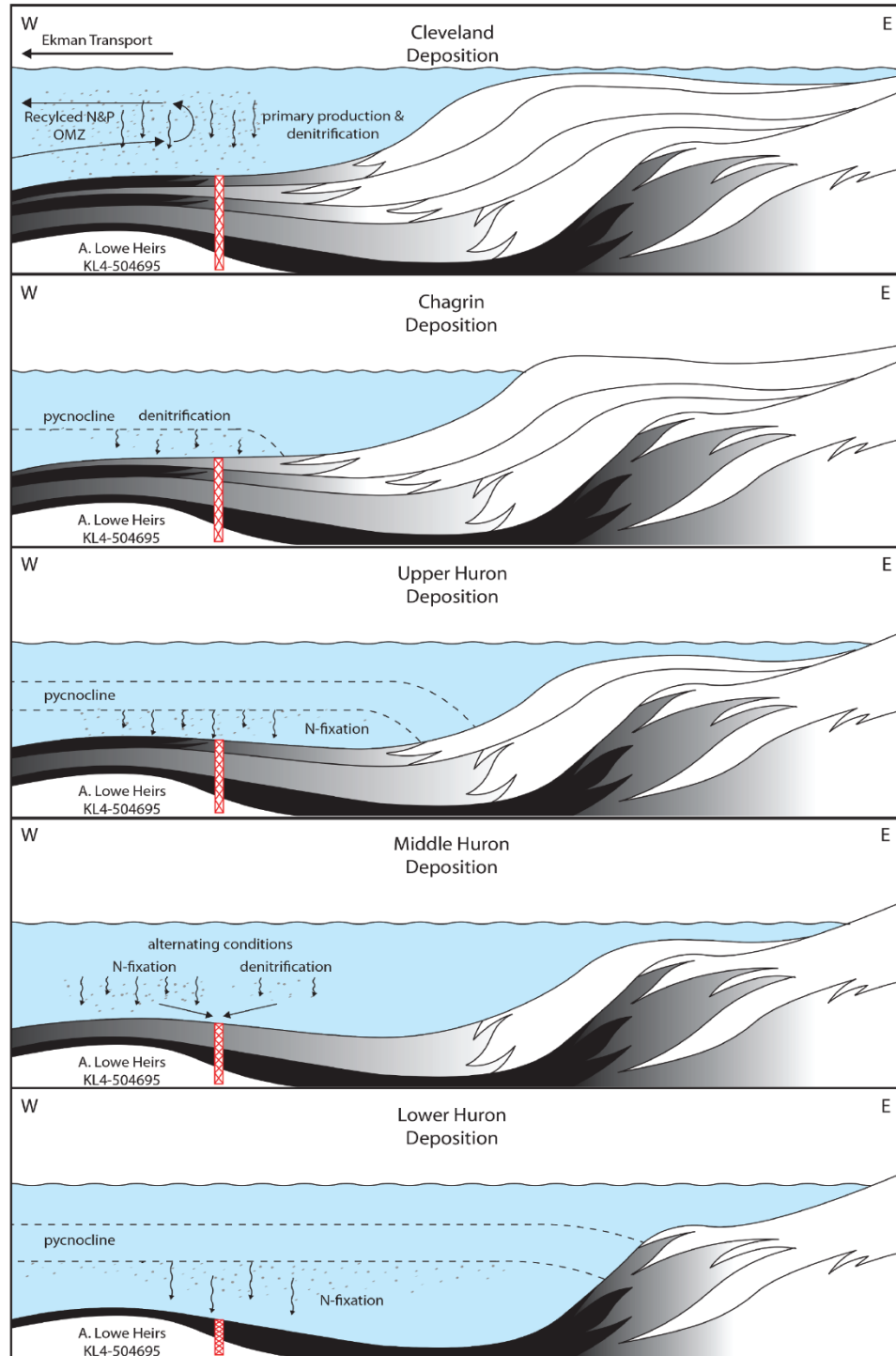


Figure 11. Schematic diagram using  $\delta^{15}\text{N}_{\text{bulk}}$  and TOC as proxies for oxygen concentration and OM preservation. Arrows show the generalized evolution of paleoredox conditions during Ohio Shale deposition.

One exception does exist within the Chagrin, expressed by lower  $\delta^{15}\text{N}_{\text{bulk}}$  values and increase in TOC at an approximate depth of 915 m. The Cleveland equivalent does not geochemically behave in the same manner as other transgressive lower and upper Huron shale members. The Cleveland equivalent is characterized by high TOC and the progressive increase in  $\delta^{15}\text{N}_{\text{bulk}}$  values are the greatest encountered throughout the entire Ohio Shale. This suggests suboxic water column conditions, denitrification, and OM preservation during the Cleveland equivalent deposition: which is atypical compared to true Cleveland black shale depositional interpretations. Geochemical studies by Ettensohn *et al.* (1988) and Robl and Barron (1988) were the first to suggest Cleveland black shale deposition was deposited under upwelling conditions; however, their sample locations were restricted to central Kentucky along the flank of the Cincinnati Arch. Our study site is located further east more proximal to the prograding Chagrin shelf. Schmoker (1981) concluded that the Cleveland Member is approximately 200 gamma ray API units below normal in southeastern Kentucky even though concentrations of TOC



EXPLANATION

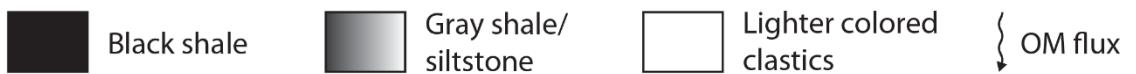


Figure 12. Synthetic depositional model for individual members of the Ohio Shale

are high. The lack of correlation between gamma ray signals and TOC may be due to high sedimentation rates and/or bioturbation and the remobilization of uranium (Kepferle, 1993; Zheng *et al.*, 2002; Lüning and Kolonic, 2003; Morford *et al.*, 2009). Furthermore, studies adjacent to Pike County, Kentucky, in West Virginia, have proven the Cleveland grades into a gray shale siltstone that is undistinguishable and “undifferentiated” from Chagrin facies (Neal, 1979; Hohn *et al.*, 1980). Increased fluvial input and the progradation of greenish-gray shale facies may have disrupted upwelling as suggested by depositional models by Ettensohn and Barron (1981), especially locations nearest to the Chagrin shelf. After the deposition of the upper Huron Member, there is a progressively fining-upward trend through the Mississippian Bedford-Berea fluvial clastics, as indicated by the gamma ray log (Fig. 5). This suggests that at our particular site of deposition, the Cleveland equivalent represents flych-like sedimentation compared to true Cleveland black shale deposition in an oxygen minimum zone (OMZ) more westwardly in central Kentucky. Geochemical data for our study site in Pike County, Kentucky suggests the Cleveland equivalent was deposited proximal to upwelling conditions but not within the OMZ (Fig. 12); the proximity to the OMZ led to elevated rates of primary production and subsequent high TOC contents found within the Cleveland equivalent.

## 5.2 Other geochemical proxies

Other geochemical proxies ( $\delta^{13}\text{C}_{\text{org}}$  and  $\text{C}_{\text{org}}/\text{TN}$ ) can be used to strengthen our depositional environment interpretations. There is a correlation between sedimentary  $\delta^{15}\text{N}_{\text{bulk}}$  values,  $\text{C}_{\text{org}}/\text{TN}$  and,  $\delta^{13}\text{C}_{\text{org}}$ . Low  $\delta^{15}\text{N}_{\text{bulk}}$  suggests anoxia and higher preservation of OM, which coincides with high  $\text{C}_{\text{org}}/\text{TN}$ ; in contrast, high  $\delta^{15}\text{N}_{\text{bulk}}$  values

is indicative of suboxia, which coincides with minimal OM preservation and low  $C_{org}/TN$ . The only exception exists within the Cleveland equivalent member, which is characterized by high  $\delta^{15}N_{bulk}$  and  $C_{org}/TN$  due to being deposited in suboxic conditions in close proximity to upwelling conditions.

Organic carbon isotope ratios have predominately been used to differentiate between marine and terrestrial OM. Maynard (1981) used  $\delta^{13}C_{org}$  as an indicator for dispersal patterns of terrestrial and marine OM in the Ohio Shale and its equivalents. He concluded that non-marine OM (coal) has a  $\delta^{13}C_{org}$  value of approximately -25‰, while basinal black shale samples had values near -30.5‰. However, there are some caveats to the findings of Maynard (1981), some of which the author mentions: (1) the more than 130 samples of Ohio Shale and age-equivalent units were taken from 6 states spanning from New York to Tennessee and averaged over the entire Appalachian Basin; thus, samples from other states may not represent the  $\delta^{13}C_{org}$  of the true Ohio Shale which is only recognized in Ohio and Kentucky; (2) photosynthetic plankton encompass a large range of  $\delta^{13}C_{org}$  values from -10 to -31‰ (Bickert, 2006); and (3) it was assumed that  $\delta^{13}C_{org}$  values are solely dependent on OM source. If the same end member  $\delta^{13}C_{org}$  values from Maynard (1981) were applied to our data, it would suggest that there are major contributions of both marine and terrestrial OM in the Ohio Shale in Pike County, Kentucky. Rock-Eval pyrolysis studies by Ingall *et al.* (1993), Rimmer *et al.* (1993), and Ryder *et al.* (2013) have proven that the Ohio Shale in the eastern Kentucky and the New Albany Shale in the adjacent Illinois Basin contain predominantly type II kerogen associated with high hydrogen indices and moderate oxygen indices, reflecting predominant marine OM sources. These studies also suggested that Ohio Shale and New



Albany samples that are characterized by lower hydrogen and higher oxygen indices could either be due to oxidation of type II OM during deposition or conversion of type II kerogen to solid bitumen during thermal degradation.

Therefore, the variations in  $\delta^{13}\text{C}_{\text{org}}$  values must reflect other mechanisms. Multiple studies (e.g. Hollander and McKenzie, 1991; Hodell and Schelske, 1998; Kump and Arthur, 1999; Popp *et al.*, 1997; Schubert and Calvert, 2001; Jarvis *et al.*, 2011) have shown that  $\text{CO}_2$  acts as an integrator during carbon isotopic fractionation during aqueous photosynthesis. Availability of  $\text{CO}_2$  in response to changes in the partial pressure of carbon dioxide ( $\text{pCO}_2$ ) have the potential to affect the carbon reservoir and  $\delta^{13}\text{C}_{\text{org}}$  signal in OM. Photosynthetic organisms typically discriminate in against  $^{13}\text{C}$  during photosynthesis when  $\text{pCO}_2$  is high (Kump and Arthur, 1999; Jarvis *et al.*, 2011); however, when  $\text{pCO}_2$  is lowered,  $\text{CO}_{2(\text{aqueous})}$  is limited due to restricted exchange between the aqueous and atmospheric  $\text{CO}_2$  pools, and photosynthetic organisms discriminate less against  $^{13}\text{C}$  and  $\delta^{13}\text{C}_{\text{org}}$  becomes progressively enriched (Hodell and Schelske, 1998; Schubert and Calvert, 2001). Instead of suggesting changes in types of OM,  $\delta^{13}\text{C}_{\text{org}}$  values in this research likely reflect variations in  $\text{pCO}_2$  and  $\text{CO}_{2(\text{aqueous})}$  possible driven by third order eustatic events.

### *5.3 Validity of depositional environment interpretations*

This research was conducted from well cuttings from the A. Lowe Heirs KL4-504695 at approximately 3 m intervals, so there is some concern about discrepancies and inaccuracies due to sample depth calibration and possible sample contamination. Geochemical profiles need to be lithostratigraphically correlated in order to support the

validity of our depositional environment interpretations. In theory, there should be an antithetic relationship between gamma ray signals and  $\delta^{15}\text{N}_{\text{bulk}}$  values for a particular interval, with lower  $\delta^{15}\text{N}_{\text{bulk}}$  values correlating to higher gamma ray signal, indicating anoxic darker shale deposition and higher  $\delta^{15}\text{N}_{\text{bulk}}$  with lower gamma ray signals reflecting suboxic lighter shale deposition. This antithetic relationship between  $\delta^{15}\text{N}_{\text{bulk}}$  and gamma ray signals is seen in our data set (Fig. 10), which supports our depositional interpretations since geochemical data matches the lithostratigraphy.

#### *5.4 Relationship between $\delta^{15}\text{N}_{\text{bulk}}$ and $\delta^{15}\text{N}_{\text{inorg}}$*

Now that the paleoredox conditions and evolution of each Ohio Shale member have been established, it is possible to evaluate the relationships between paleoredox-dependent  $\delta^{15}\text{N}_{\text{bulk}}$  and  $\delta^{15}\text{N}_{\text{inorg}}$ . Along with characterizing the paleoredox conditions of the Ohio Shale, another goal was to evaluate the driving mechanism(s) responsible for the observed relationships between  $\delta^{15}\text{N}_{\text{bulk}}$  and  $\delta^{15}\text{N}_{\text{inorg}}$  through the core. Three conceptual scenarios exist between  $\delta^{15}\text{N}_{\text{bulk}}$  and  $\delta^{15}\text{N}_{\text{inorg}}$  values as shown in Figure 10: (1)  $\delta^{15}\text{N}_{\text{bulk}} > \delta^{15}\text{N}_{\text{inorg}}$  (positive), (2)  $\delta^{15}\text{N}_{\text{bulk}} < \delta^{15}\text{N}_{\text{inorg}}$  (negative), or (3)  $\delta^{15}\text{N}_{\text{bulk}} \approx \delta^{15}\text{N}_{\text{inorg}}$  (closed). In general, there is a correlation between crossover profiles and the original paleoredox conditions; positive crossovers ( $\delta^{15}\text{N}_{\text{bulk}} > \delta^{15}\text{N}_{\text{inorg}}$ ; shaded blue) are associated with anoxic intervals, while negative crossovers ( $\delta^{15}\text{N}_{\text{bulk}} < \delta^{15}\text{N}_{\text{inorg}}$ ; shaded gray) are associated with suboxic intervals. Although there is a correlation between the original redox condition and crossover profiles, subsequent diagenetic and catagenetic processes need to be taken into account to fully evaluate the relationship between  $\delta^{15}\text{N}_{\text{inorg}}$  with respect to  $\delta^{15}\text{N}_{\text{bulk}}$  values.

#### 5.4.1 Implications of negative ( $\delta^{15}\text{N}_{\text{bulk}} < \delta^{15}\text{N}_{\text{inorg}}$ ) crossover profiles

Negative crossover profiles are associated with anoxic intervals, characterized by higher gamma ray signals (typically greater than 220 API), and high TOC and IN concentrations (Fig. 10). The fact that  $\delta^{15}\text{N}_{\text{inorg}}$  values are higher than  $\delta^{15}\text{N}_{\text{bulk}}$  is contradictory with regards to isotopic fractionation kinetics described for the thermal degradation of OM and the transformation into aqueous  $\text{NH}_4^+$  as thermal degradation during catagenesis results in the preferential release of light  $^{14}\text{NH}_4^+$  isotope (Williams *et al.* 1995; Freudenthal *et al.*, 2001; Mingram and Braüer, 2001; Plessen *et al.*, 2010). Therefore, higher  $\delta^{15}\text{N}_{\text{inorg}}$  values with respect to  $\delta^{15}\text{N}_{\text{bulk}}$  suggests: (1) isotopic buffering must occur during the thermal transformation of OM to aqueous  $\text{NH}_4^+$ , releasing both isotopically light  $^{14}\text{NH}_4^+$  and heavy  $^{15}\text{NH}_4^+$ ; and (2) there is an overall preferential uptake and fixation of  $^{15}\text{NH}_4^+$  by authigenic clays compared to  $^{14}\text{NH}_4^+$ . Diagenetic processes need to be taken into account to understand how isotopic buffering and preferential fixation of  $^{15}\text{NH}_4^+$  by authigenic clays during catagenesis is ascertained.

The degradation-recondensation processes of OM play a crucial role in achieving isotopic buffering. Anoxia promotes greater quantities of OM preservation and subjects sediments to mineralization and anaerobic biodegradation. These processes breakdown macromolecular components into simple molecules which can be used by heterotrophs (Killops and Killops, 2005); however, large clay contents (characterized by higher gamma ray signals due to adsorption of naturally radioactive elements), offer protection to amorphous, labile molecules from complete microbial degradation (Largeau and Derenne, 1993; Wu *et al.*, 2012 and references therein) by preservative mechanisms described by Kennedy *et al.* (2014 and references therein). Furthermore, clays

catalytically promote the structural rearrangement of ON components, such as pyridine and pyrrole (Behar and Vandenbroucke, 1987; Ader *et al.*, 2006; Vandenbroucke and Largeau, 2007), into more structurally and thermally stable ON heterocycles and humic complexes (Boudou *et al.*, 2008) due to processes similar to natural humification (Wu *et al.*, 2012 and references therein). The structural rearrangement into thermally stable ON heterocycles, such as N-C<sub>3</sub> cyclazines, is crucial because it promotes isotopic buffering during the thermal degradation of OM to aqueous NH<sub>4</sub><sup>+</sup> (Boudou *et al.*, 2008), resulting in the release of both isotopically light and heavy NH<sub>4</sub><sup>+</sup>. Laboratory studies by Karamanos and Rennie (1978) suggested that after chemical equilibrium is achieved, clays preferentially fix <sup>15</sup>NH<sub>4</sub><sup>+</sup> due to the excess of <sup>15</sup>NH<sub>4</sub><sup>+</sup> in solution. Over geologic time, isotopically heavy <sup>15</sup>NH<sub>4</sub><sup>+</sup> would be fixed by surrounding authigenic clays, resulting in a negative crossover profile for anoxic intervals (Fig. 13).

#### 5.4.2 Implications of positive ( $\delta^{15}N_{bulk} > \delta^{15}N_{inorg}$ ) crossover profiles

Positive crossover profiles are associated with suboxic intervals, characterized by lower gamma ray signals (typically less than 220 API), and low TOC and IN concentrations (Fig. 10). Lower  $\delta^{15}N_{inorg}$  values with respect to  $\delta^{15}N_{bulk}$  suggests normal fractionation kinetics prevail during the thermal degradation of OM to aqueous NH<sub>4</sub><sup>+</sup>: releasing isotopically light <sup>14</sup>NH<sub>4</sub><sup>+</sup> which is then fixed by authigenic clays.

Suboxic conditions promote rapid decomposition of OM via mineralization and aerobic degradation, reflected by minimal TOC and C<sub>org</sub>/TN values. Compared to anoxic intervals, suboxic intervals including the Cleveland equivalent generally have lower clay

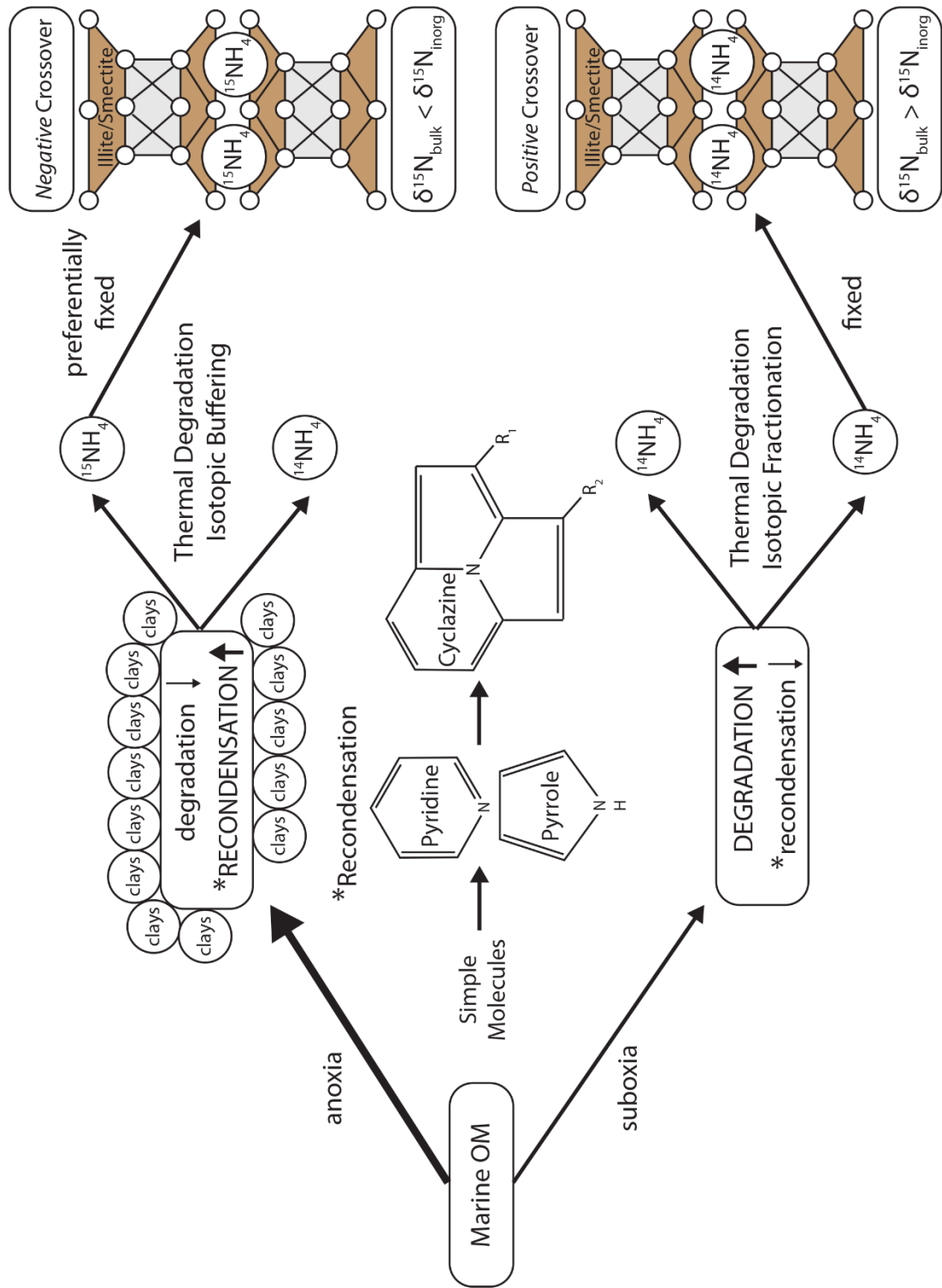


Figure 13. Schematic diagram explaining the diagenetic/catagenetic processes and mechanisms responsible for negative and positive crossover profiles. Thickness of arrows is in regards to the relative intensity of a particular process. The asterisk (\*) denotes the recondensation process responsible for the generation of thermally stable cyclazine ON heterocycles and isotopic buffering during the thermal degradation of OM and the transformation to aqueous  $\text{NH}_4^+$ .

contents, as indicated by lower gamma ray signals. The lower abundance of clays inhibits the degradation-recondensation process, which is responsible for the protection of simple molecules from complete microbial degradation and the formation of thermally stable ON heterocycles required for isotopic buffering during thermal degradation. Upon catagenesis, normal isotopic fractionation kinetics prevail during the thermal transformation of OM, and isotopically light  $^{14}\text{NH}_4^+$  released and fixed by surrounding authigenic clays: resulting in a positive crossover profile for suboxic intervals (Fig. 13).

#### 5.4.3 Implications of closed ( $\delta^{15}\text{N}_{\text{bulk}} \approx \delta^{15}\text{N}_{\text{inorg}}$ ) intervals

The fact that closed intervals, those characterized by  $\delta^{15}\text{N}_{\text{bulk}} \approx \delta^{15}\text{N}_{\text{inorg}}$ , occur tells us something related to the catagenetic process of fluid flow and the overall fracture network of an unconventional system. This suggests that isotopic equilibrium exchange is occurring within a compartmentalized unit. Williams *et al.* (1995) noted that mudstones act as a closed system, *except* along fractures, where  $\text{NH}_4^+$  derived from the local OM could be incorporated in authigenic clays with little isotopic fractionation. Exchange between reactive inorganic nitrogen in circulating formation fluids with stationary OM pools results in the overall isotopic buffering of  $\delta^{15}\text{N}$  values: reducing the variability between separate nitrogen isotopic species in thermally mature stratigraphic sequences (Schimmelmann and Lis, 2010). These compartmentalized zones possess an internal microscopic fracture network within the compartmentalized unit, allowing isotopic equilibrium exchange between different forms of nitrogen, resulting in approximately equal bulk and inorganic nitrogen isotopic values (Fig. 14). When comparing  $\delta^{15}\text{N}_{\text{bulk}}$  and  $\delta^{15}\text{N}_{\text{inorganic}}$  profiles with the gamma ray log (Fig. 10), closed intervals occur in

stratigraphic zones characterized by decreased gamma ray values (decreased clay content) while being sealed above and below by gamma ray spikes, suggesting closed intervals are sealed by impermeable shales units.

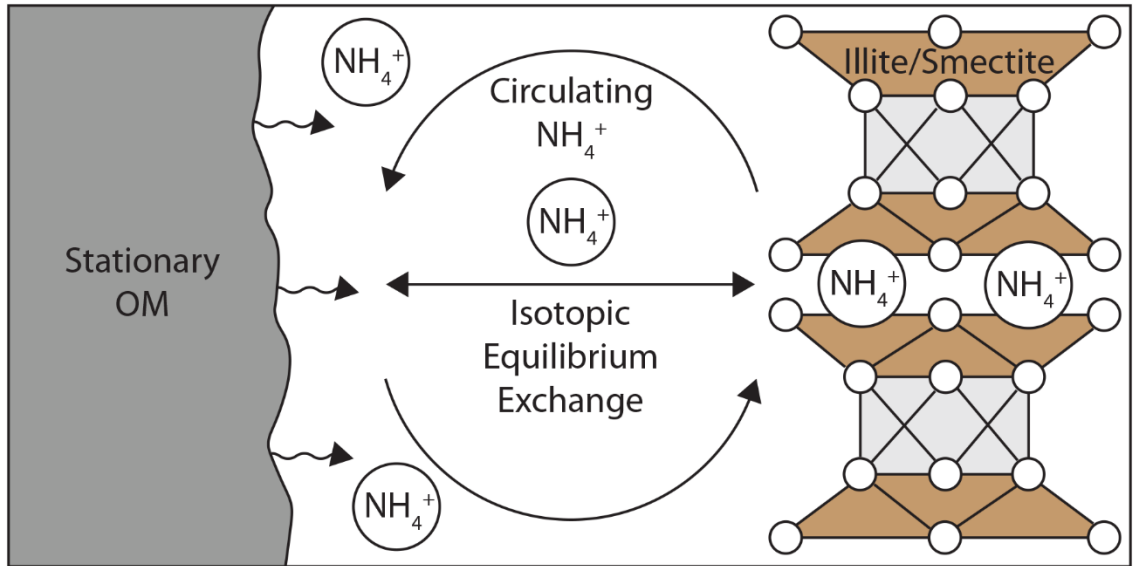


Figure 104. Schematic diagram illustrating isotopic equilibrium exchange between stationary OM and circulating  $\text{NH}_4^+$  within a compartmentalized interval

## CHAPTER VI

### CONCLUSIONS

In the A. Lower Heirs KL4-504695 in Pike County,  $\delta^{15}\text{N}_{\text{bulk}}$  and other complementary geochemical proxies have proven useful for characterizing the paleoredox evolution of the Ohio Shale depositional environment. The lower Huron Member was deposited in anoxic conditions beneath the pycnocline, and is the only Ohio Shale member to display black shale qualities at this particular locale while succeeding members reflect flysch-like clastic deposition. The middle Huron was deposited in alternating suboxic and anoxic conditions, suggesting deposition at this particular site fluctuated within the pycnocline and below it. The upper Huron Member was deposited under anoxic conditions below the pycnocline. Following the upper Huron, the Chagrin Member was deposited in a predominantly suboxic environment within the pycnocline, although one exception does exist. While upwelling conditions were prevalent during latest Famennian, the Cleveland equivalent in Pike County, Kentucky was deposited proximal to upwelling conditions, but not within the OMZ responsible for true black shale deposition. Although inaccuracies are associated with well cutting sample collection, the geochemical data presented matches the lithostratigraphy in the gamma ray log: validating our depositional environment interpretations.

After establishing the paleoredox conditions of the Ohio Shale, it is possible to



evaluate the mechanisms and conditions responsible for the relationship between  $\delta^{15}\text{N}_{\text{bulk}}$  and  $\delta^{15}\text{N}_{\text{inorg}}$  values. There appears to be an intricate relationship between paleoredox conditions, degradation-recondensation processes, clay contents, and diagenetic/catagenetic processes. Negative crossover profiles, associated with anoxic intervals, suggests that isotopic buffering is occurring along with an observed inversion of normal fractionation kinetics during thermal degradation of OM, and there is a preferential uptake of heavy  $^{15}\text{NH}_4^+$  by authigenic clays. Isotopic buffering is achieved during degradation-recondensation processes, in which clays promote the structural rearrangement of simple molecules into thermally stable ON (cyclazine) heterocycles. Upon thermal degradation, isotopically light and heavy  $\text{NH}_4^+$  is released, and over geological time  $^{15}\text{NH}_4^+$  is preferentially fixed by authigenic clays, resulting in a negative crossover profile. Positive crossover profiles, associated with suboxic conditions, suggest that normal isotopic fractionation kinetics prevails, releasing isotopically light  $^{14}\text{NH}_4^+$  during the thermal degradation of OM. This is achieved due to the lower clay contents which hinders the recondensation processes responsible for the generation of thermally stable ON heterocycles required for isotopic buffering during thermal degradation. Therefore, isotopic fractionation occurs and releases isotopically light  $^{14}\text{NH}_4^+$  which is then fixed by authigenic clays: resulting in a positive crossover profile. Closed intervals are related to the overall fracture network and associated with compartmentalization within a particular interval. Isotopic equilibrium exchange between stationary OM and circulating aqueous  $\text{NH}_4^+$  pools results in the mutual equivalent  $\delta^{15}\text{N}_{\text{bulk}}$  and  $\delta^{15}\text{N}_{\text{inorg}}$  values within the compartmentalized interval.

### 6.1 Recommendations

Further studies on well cutting samples from the A. Lowe Heirs KL4-504695 from Pike County, Kentucky should include x-ray diffraction (XRD) analyses. XRD would allow one to identify and quantify the different types minerals present throughout the Ohio Shale. Different clay minerals have different affinities for adsorbing and fixing  $\text{NH}_4^+$  as it is thermally released during catagenesis. Also, it is recommended that the same X-ray photoelectron spectroscopy (XPS) techniques utilized by Boudou *et al.* (2008) should be conducted. This will allow us to characterize XPS peaks to structural ON moieties (e.g. pyridinic-N, pyrrolic-N, and cyclazines). Although it is mentioned that cyclazines are typically associated with higher metamorphic grade sediments, it was noted by references within Boudou *et al.* (2008 and references therein) that humic cyclazine complexes can spontaneous form at low temperatures.

## REFERENCES

- Ader, M., P. Cartigny, J.-P. Boudou, J.-H. Oh, E. Petit, and M. Javoy, 2006, Nitrogen isotopic evolution of carbonaceous matter during metamorphism: Methodology and preliminary results: *Chemical Geology*, v. 232, p. 152-169.
- Altabet, M. A., and R. Francois, 1994, Sedimentary nitrogen isotopic ratio as a recorder for surface ocean nitrate utilization: *Global Biogeochemical Cycles*, v. 8, p. 103-116.
- Beaumont, V. I., L. L. Jahnke, and D. J. Des Marais, 2000, Nitrogen isotopic fractionation in the synthesis of photosynthetic pigments in *Rhodobacter capsulatus* and *Anabaena cylindrica*: *Organic Geochemistry*, v. 31, p. 1075-1085.
- Behar, F., and M. Vandenbroucke, 1987, Chemical modelling of kerogens: *Organic Geochemistry*, v. 11, p. 15-24.
- Bickert, T., 2006, Influence of Geochemical Processes on Stable Isotope Distribution in Marine Sediments, in H. Schulz, and M. Zabel, eds., *Marine Geochemistry*, Springer Berlin Heidelberg, p. 339-369.
- Boudou, J.-P., A. Schimmelmann, M. Ader, M. Mastalerz, M. Sebiló, and L. Gengembre, 2008, Organic nitrogen chemistry during low-grade metamorphism: *Geochimica et Cosmochimica Acta*, v. 72, p. 1199-1221.

- Bremner, J. M., and D. R. Keeney, 1966, Determination and Isotope-Ratio Analysis of Different Forms of Nitrogen in Soils: 3. Exchangeable Ammonium, Nitrate, and Nitrite by Extraction-Distillation Methods1: *Soil Science Society of America Journal*, v. 30, p. 577-582.
- Brezinski, D. K., C. B. Cecil, V. W. Skema, and C. A. Kertis, 2009, Evidence for long-term climate change in Upper Devonian strata of the central Appalachians: *Palaeogeography, Palaeoclimatology, Palaeoecology*, v. 284, p. 315-325.
- Brezinski, D. K., C. B. Cecil, V. W. Skema, and R. Stamm, 2008, Late Devonian glacial deposits from the eastern United States signal an end of the mid-Paleozoic warm period: *Palaeogeography, Palaeoclimatology, Palaeoecology*, v. 268, p. 143-151.
- Brunner, B., S. Contreras, M. F. Lehmann, O. Matantseva, M. Rollog, T. Kalvelage, G. Klockgether, G. Lavik, M. S. M. Jetten, B. Kartal, and M. M. M. Kuypers, 2013, Nitrogen isotope effects induced by anammox bacteria: *Proceedings of the National Academy of Sciences*, v. 110, p. 18994-18999.
- Calvert, S. E., and T. F. Pedersen, 1993, Geochemistry of Recent oxic and anoxic marine sediments: Implications for the geological record: *Marine Geology*, v. 113, p. 67-88.
- Carpenter, E. J., H. R. Harvey, B. Fry, and D. G. Capone, 1997, Biogeochemical tracers of the marine cyanobacterium *Trichodesmium*: *Deep Sea Research Part I: Oceanographic Research Papers*, v. 44, p. 27-38.
- Carter, J., and V. Barwick, 2011, Good Practice Guide for Isotope Ratio Mass Spectrometry, Forensic Isotope Ratio Mass Spectrometry Network, p. 48.

- Casciotti, K. L., C. Buchwald, A. E. Santoro, and C. Frame, 2011, Chapter eleven - Assessment of Nitrogen and Oxygen Isotopic Fractionation During Nitrification and Its Expression in the Marine Environment, *in* G. K. Martin, ed., *Methods in Enzymology*, v. Volume 486, Academic Press, p. 253-280.
- Cheatham, M. M., W. F. Sangrey, and W. M. White, 1993, Sources of error in external calibration ICP-MS analysis of geological samples and an improved non-linear drift correction procedure: *Spectrochimica Acta Part B: Atomic Spectroscopy*, v. 48, p. 487-506.
- Checkley Jr, D. M., and C. A. Miller, 1989, Nitrogen isotope fractionation by oceanic zooplankton: *Deep Sea Research Part A. Oceanographic Research Papers*, v. 36, p. 1449-1456.
- Codispoti, L. A., J. A. Brandes, J. P. Christensen, A. H. Devol, S. W. A. Naqvi, H. W. Paerl, and T. Yoshinari, 2001, The oceanic fixed nitrogen and nitrous oxide budgets: Moving targets as we enter the anthropocene?: *Scientia Marina*, v. 65.
- Compton, J. S., L. B. Williams, and R. E. Ferrell Jr, 1992, Mineralization of organogenic ammonium in the Monterey Formation, Santa Maria and San Joaquin basins, California, USA: *Geochimica et Cosmochimica Acta*, v. 56, p. 1979-1991.
- de Lange, G. J., 1992, Distribution of exchangeable, fixed, organic and total nitrogen in interbedded turbiditic/pelagic sediments of the Madeira Abyssal Plain, eastern North Atlantic: *Marine Geology*, v. 109, p. 95-114.
- de Witt Jr., W., J. B. Roen, and L. G. Wallace, 1993, Stratigraphy of Devonian black shales and associated rocks in the Appalachian Basin, *in* J. B. Roen, and R. C.

- Kepferle, eds., Petroleum Geology of the Devonian and Mississippian Black Shale of Eastern North America, p. B1-B57.
- Delwiche, C. C., and P. L. Steyn, 1970, Nitrogen isotope fractionation in soils and microbial reactions: *Environmental Science & Technology*, v. 4, p. 929-935.
- Devol, A. H., 2008, Chapter 6 - Denitrification Including Anammox, in D. G. Capone, D. A. Bronk, M. R. Mulholland, and E. J. Carpenter, eds., Nitrogen in the Marine Environment (2nd Edition): San Diego, Academic Press, p. 263-301.
- Drits, V. A., H. Lindgreen, and A. L. Salyn, 1997, Determination of the content and distribution of fixed ammonium in illite-smectite by X-ray diffraction: Application to North Sea illite-smectite: *American Mineralogist*, v. 82, p. 79-87.
- Ettensohn, F. R., 1987, Rates of Relative Plate Motion during the Acadian Orogeny Based on the Spatial Distribution of Black Shales: *The Journal of Geology*, v. 95, p. 572-582.
- Ettensohn, F. R., 1992, Controls on the origin of the Devonian-Mississippian oil and gas shales, east-central United States: *Fuel*, v. 71, p. 1487-1492.
- Ettensohn, F. R., 2008, Chapter 4 The Appalachian Foreland Basin in Eastern United States, in D. M. Andrew, ed., Sedimentary Basins of the World, v. 5, Elsevier, p. 105-179.
- Ettensohn, F. R., and L. S. Barron, 1981, Depositional model for the Devonian-Mississippian black-shale sequence of North America: a tectono-climatic approach, Morgantown, West Virginia, United States Department of Energy.

- Ettensohn, F. R., and T. D. Elam, 1985, Defining the nature and location of a Late Devonian–Early Mississippian pycnocline in eastern Kentucky: *Geological Society of America Bulletin*, v. 96, p. 1313-1321.
- Ettensohn, F. R., M. Miller, S. Dillman, T. Elam, K. Geller, D. Swager, G. Markowitz, R. Woock, and L. Barron, 1988, Characterization and implications of the Devonian–Mississippian black shale sequence, eastern and central Kentucky, USA: Pycnoclines, transgression, regression, and tectonism: Devonian of the World: Proceedings of the 2nd International Symposium on the Devonian System — Memoir 14, p. 323-345.
- Filer, J. K., 2002, Late Frasnian sedimentation cycles in the Appalachian basin—possible evidence for high frequency eustatic sea-level changes: *Sedimentary Geology*, v. 154, p. 31-52.
- Freudenthal, T., T. Wagner, F. Wenzhöfer, M. Zabel, and G. Wefer, 2001, Early diagenesis of organic matter from sediments of the eastern subtropical Atlantic: evidence from stable nitrogen and carbon isotopes: *Geochimica et Cosmochimica Acta*, v. 65, p. 1795-1808.
- Galbraith, E. D., D. M. Sigman, R. S. Robinson, and T. F. Pedersen, 2008, Chapter 34 - Nitrogen in Past Marine Environments, in D. G. Capone, D. A. Bronk, M. R. Mulholland, and E. J. Carpenter, eds., *Nitrogen in the Marine Environment* (2nd Edition): San Diego, Academic Press, p. 1497-1535.
- Godfrey, L. V., and J. B. Glass, 2011, Chapter twenty-two - The Geochemical Record of the Ancient Nitrogen Cycle, Nitrogen Isotopes, and Metal Cofactors, in G. K.

- Martin, ed., *Methods in Enzymology*, v. Volume 486, Academic Press, p. 483-506.
- Gruber, N., 2008, Chapter 1 - The Marine Nitrogen Cycle: Overview and Challenges, *in* D. G. Capone, D. A. Bronk, M. R. Mulholland, and E. J. Carpenter, eds., *Nitrogen in the Marine Environment (2nd Edition)*: San Diego, Academic Press, p. 1-50.
- Haq, B. U., and S. R. Schutter, 2008, A Chronology of Paleozoic Sea-Level Changes: *Science*, v. 322, p. 64-68.
- Hodell, D. A., and C. L. Schelske, 1998, Production, sedimentation, and isotopic composition of organic matter in Lake Ontario: *Limnology and Oceanography*, v. 43, p. 200-214.
- Hoering, T., 1955, Variations of Nitrogen-15 Abundance in Naturally Occurring Substances: *Science*, v. 122, p. 1233-1234.
- Hohn, M. E., D. W. Neal, and J. Renton, 1980, Inorganic Geochemistry of Devonian Shales in southern West Virginia: Geographic and Stratigraphic Trends, Morgantown, West Virginia, West Virginia Geological and Economic Survey, p. 34.
- Hollander, D. J., and J. A. McKenzie, 1991, CO<sub>2</sub> control on carbon-isotope fractionation during aqueous photosynthesis: A paleo-pCO<sub>2</sub> barometer: *Geology*, v. 19, p. 929-932.
- Holmes, M. E., P. J. Müller, R. R. Schneider, M. Segl, J. Pätzold, and G. Wefer, 1996, Stable nitrogen isotopes in Angola Basin surface sediments: *Marine Geology*, v. 134, p. 1-12.
- Hunt, J. M., 1979, *Petroleum Geochemistry and Geology*, W.H. Freeman.



- Ingall, E. D., R. M. Bustin, and P. Van Cappellen, 1993, Influence of water column anoxia on the burial and preservation of carbon and phosphorus in marine shales: *Geochimica et Cosmochimica Acta*, v. 57, p. 303-316.
- Isaacson, P. E., E. Díaz-Martínez, G. W. Grader, J. Kalvoda, O. Babek, and F. X. Devuyt, 2008, Late Devonian–earliest Mississippian glaciation in Gondwanaland and its biogeographic consequences: *Palaeogeography, Palaeoclimatology, Palaeoecology*, v. 268, p. 126-142.
- Jarvis, I., J. S. Lignum, D. R. Gröcke, H. C. Jenkyns, and M. A. Pearce, 2011, Black shale deposition, atmospheric CO<sub>2</sub> drawdown, and cooling during the Cenomanian-Turonian Oceanic Anoxic Event: *Paleoceanography*, v. 26, p. n/a-n/a.
- Jetten, M. S. M., M. Wagner, J. Fuerst, M. van Loosdrecht, G. Kuenen, and M. Strous, 2001, Microbiology and application of the anaerobic ammonium oxidation ('anammox') process: *Current Opinion in Biotechnology*, v. 12, p. 283-288.
- Jia, Y., 2006, Nitrogen isotope fractionations during progressive metamorphism: A case study from the Paleozoic Cooma metasedimentary complex, southeastern Australia: *Geochimica et Cosmochimica Acta*, v. 70, p. 5201-5214.
- Johnson, J. G., G. Klapper, and C. A. Sandberg, 1985, Devonian eustatic fluctuations in Euramerica: *Geological Society of America Bulletin*, v. 96, p. 567-587.
- Junium, C. K., and M. A. Arthur, 2007, Nitrogen cycling during the Cretaceous, Cenomanian-Turonian Oceanic Anoxic Event II: *Geochemistry, Geophysics, Geosystems*, v. 8, p. Q03002.

- Karamanos, R. E., and D. A. Rennie, 1978, Nitrogen Isotope Fractionation During Ammonium Exchange Reactions with Soil Clay: *Canadian Journal of Soil Science*, v. 58, p. 53-60.
- Karl, D. M., and A. F. Michaels, 2001, Nitrogen Cycle, in J. H. Steele, ed., *Encyclopedia of Ocean Sciences*: Oxford, Academic Press, p. 1876-1884.
- Kennedy, M. J., S. C. Löhr, S. A. Fraser, and E. T. Baruch, 2014, Direct evidence for organic carbon preservation as clay-organic nanocomposites in a Devonian black shale; from deposition to diagenesis: *Earth and Planetary Science Letters*, v. 388, p. 59-70.
- Kepferle, R. C., 1993, A Depositional Model and Basin Analysis for the Gas-Bearing Black Shale (Devonian and Mississippian) in the Appalachian Basin, in J. B. Roen, and R. C. Kepferle, eds., *Petroleum Geology of the Devonian and Mississippian Black Shale of Eastern North America*, p. F1-F23.
- Killops, S., and V. Killops, 2004, Chemical Composition of Organic Matter, Introduction to Organic Geochemistry, Blackwell Publishing Ltd., p. 30-70.
- Killops, S., and V. Killops, 2004, Production, Preservation and Degradation of Organic Matter, Introduction to Organic Geochemistry, Blackwell Publishing Ltd., p. 71-116.
- Krooss, B. M., R. Littke, B. Müller, J. Frielingsdorf, K. Schwochau, and E. F. Idiz, 1995, Generation of nitrogen and methane from sedimentary organic matter: Implications on the dynamics of natural gas accumulations: *Chemical Geology*, v. 126, p. 291-318.

- Kump, L. R., and M. A. Arthur, 1999, Interpreting carbon-isotope excursions: carbonates and organic matter: *Chemical Geology*, v. 161, p. 181-198.
- Kuypers, M. M. M., G. Lavik, D. Woebken, M. Schmid, B. M. Fuchs, R. Amann, B. B. Jørgensen, and M. S. M. Jetten, 2005, Massive nitrogen loss from the Benguela upwelling system through anaerobic ammonium oxidation: *Proceedings of the National Academy of Sciences of the United States of America*, v. 102, p. 6478-6483.
- Largeau, C., and S. Derenne, 1993, Relative efficiency of the Selective Preservation and Degradation Recondensation pathways in kerogen formation. Source and environment influence on their contributions to type I and II kerogens: *Organic Geochemistry*, v. 20, p. 611-615.
- Lehmann, M. F., S. M. Bernasconi, A. Barbieri, and J. A. McKenzie, 2002, Preservation of organic matter and alteration of its carbon and nitrogen isotope composition during simulated and in situ early sedimentary diagenesis: *Geochimica et Cosmochimica Acta*, v. 66, p. 3573-3584.
- Lewis, T. L., and J. F. Schwietering, 1971, Distribution of the Cleveland black shale in Ohio: *Geological Society of America Bulletin*, v. 82, p. 3477-3482.
- Littke, R., B. Krooss, E. Idiz, and J. Frielingsdorf, 1995, Molecular nitrogen in natural gas accumulations: generation from sedimentary organic matter at high temperatures: *American Association of Petroleum Geologists Bulletin*, v. 79, p. 410-430.

- Lüning, S., and S. Kolonic, 2003, Uranium spectral gamma-ray response as a proxy for organic richness in black shales: Applicability and limitations: *Journal of Petroleum Geology*, v. 26, p. 153-174.
- Macko, S. A., 1981, Stable Nitrogen Isotope Ratios as Tracers of Organic Geochemical Processes: Dissertation thesis, The University of Texas at Austin, ProQuest, UMI Dissertations Publishing.
- Macko, S. A., 1989, Stable isotope organic geochemistry of sediments from the Labrador Sea (Sites 646 and 647) and Baffin Bay (Site 645), ODP Leg 105: *Proc. Ocean Drill. Program Sci. Results*, p. 209-221.
- Macko, S. A., M. H. Engel, and Y. Qian, 1994, Early diagenesis and organic matter preservation — a molecular stable carbon isotope perspective: *Chemical Geology*, v. 114, p. 365-379.
- Macko, S. A., and M. L. F. Estep, 1984, Microbial alteration of stable nitrogen and carbon isotopic compositions of organic matter: *Organic Geochemistry*, v. 6, p. 787-790.
- Maynard, J. B., 1981, Carbon isotopes as indicators of dispersal patterns in Devonian-Mississippian shales of the Appalachian Basin: *Geology*, v. 9, p. 262-265.
- McClung, W. S., K. A. Eriksson, D. O. Terry Jr, and C. A. Cuffey, 2013, Sequence stratigraphic hierarchy of the Upper Devonian Foreknobs Formation, central Appalachian Basin, USA: Evidence for transitional greenhouse to icehouse conditions: *Palaeogeography, Palaeoclimatology, Palaeoecology*, v. 387, p. 104-125.

- Meckler, A. N., G. H. Haug, D. M. Sigman, B. Plessen, L. C. Peterson, and H. R. Thierstein, 2007, Detailed sedimentary N isotope records from Cariaco Basin for Terminations I and V: Local and global implications: *Global Biogeochemical Cycles*, v. 21, p. GB4019.
- Minagawa, M., and E. Wada, 1986, Nitrogen isotope ratios of red tide organisms in the East China Sea: A characterization of biological nitrogen fixation: *Marine Chemistry*, v. 19, p. 245-259.
- Minagawa, M., D. A. Winter, and I. R. Kaplan, 1984, Comparison of Kjeldahl and combustion methods for measurement of nitrogen isotope ratios in organic matter: *Analytical Chemistry*, v. 56, p. 1859-1861.
- Mingram, B., and K. Bräuer, 2001, Ammonium concentration and nitrogen isotope composition in metasedimentary rocks from different tectonometamorphic units of the European Variscan Belt: *Geochimica et Cosmochimica Acta*, v. 65, p. 273-287.
- Mingram, B., P. Hoth, and D. E. Harlov, 2003, Nitrogen potential of Namurian shales in the North German Basin: *Journal of Geochemical Exploration*, v. 78-79, p. 405-408.
- Möbius, J., B. Gaye, N. Lahajnar, E. Bahlmann, and K.-C. Emeis, 2011, Influence of diagenesis on sedimentary  $\delta^{15}\text{N}$  in the Arabian Sea over the last 130 kyr: *Marine Geology*, v. 284, p. 127-138.
- Montoya, J. P., 2008, Chapter 29 - Nitrogen Stable Isotopes in Marine Environments, in D. G. Capone, D. A. Bronk, M. R. Mulholland, and E. J. Carpenter, eds., Nitrogen

- in the Marine Environment (2nd Edition): San Diego, Academic Press, p. 1277-1302.
- Morford, J. L., W. R. Martin, and C. M. Carney, 2009, Uranium diagenesis in sediments underlying bottom waters with high oxygen content: *Geochimica et Cosmochimica Acta*, v. 73, p. 2920-2937.
- Mulder, A., A. A. van de Graaf, L. A. Robertson, and J. G. Kuenen, 1995, Anaerobic ammonium oxidation discovered in a denitrifying fluidized bed reactor: *FEMS Microbiology Ecology*, v. 16, p. 177-183.
- Mulholland, M. R., and M. W. Lomas, 2008, Chapter 7 - Nitrogen Uptake and Assimilation, in D. G. Capone, D. A. Bronk, M. R. Mulholland, and E. J. Carpenter, eds., Nitrogen in the Marine Environment (2nd Edition): San Diego, Academic Press, p. 303-384.
- Müller, P. J., 1977, CN ratios in Pacific deep-sea sediments: Effect of inorganic ammonium and organic nitrogen compounds sorbed by clays: *Geochimica et Cosmochimica Acta*, v. 41, p. 765-776.
- Murphy, A. E., B. B. Sageman, D. J. Hollander, T. W. Lyons, and C. E. Brett, 2000, Black shale deposition and faunal overturn in the Devonian Appalachian Basin: Clastic starvation, seasonal water-column mixing, and efficient biolimiting nutrient recycling: *Paleoceanography*, v. 15, p. 280-291.
- Neal, D. W., 1979, Subsurface stratigraphy of the Middle and Upper Devonian clastic sequence in southern West Virginia and its relation to gas production: Dissertation thesis, West Virginia University, 142 p.

- Nguyen, R. T., and H. R. Harvey, 1997, Protein and amino acid cycling during phytoplankton decomposition in oxic and anoxic waters: *Organic Geochemistry*, v. 27, p. 115-128.
- Nieder, R., D. Benbi, and H. Scherer, 2011, Fixation and defixation of ammonium in soils: a review: *Biology and Fertility of Soils*, v. 47, p. 1-14.
- Papineau, D., S. J. Mojzsis, J. A. Karhu, and B. Marty, 2005, Nitrogen isotopic composition of ammoniated phyllosilicates: case studies from Precambrian metamorphosed sedimentary rocks: *Chemical Geology*, v. 216, p. 37-58.
- Pashin, J. C., and F. R. Ettensohn, 1992, Palaeoecology and sedimentology of the dysaerobic Bedford fauna (late Devonian), Ohio and Kentucky (USA): *Palaeogeography, Palaeoclimatology, Palaeoecology*, v. 91, p. 21-34.
- Pashin, J. C., and F. R. Ettensohn, 1995, Reevaluation of the Bedford-Berea Sequence in Ohio and Adjacent States: Forced Regression in a Foreland Basin: *Geological Society of America Special Papers*, v. 298, p. 1-69.
- Perkins, R. B., D. Z. Piper, and C. E. Mason, 2008, Trace-element budgets in the Ohio/Sunbury shales of Kentucky: Constraints on ocean circulation and primary productivity in the Devonian–Mississippian Appalachian Basin: *Palaeogeography, Palaeoclimatology, Palaeoecology*, v. 265, p. 14-29.
- Peters, K. E., R. E. Sweeney, and I. R. Kaplan, 1978, Correlation of carbon and nitrogen stable isotope ratios in sedimentary organic matter: *Limnology and Oceanography*, v. 23, p. 598-604.
- Plessen, B., D. E. Harlov, D. Henry, and C. V. Guidotti, 2010, Ammonium loss and nitrogen isotopic fractionation in biotite as a function of metamorphic grade in

- metapelites from western Maine, USA: *Geochimica et Cosmochimica Acta*, v. 74, p. 4759-4771.
- Popp, B. N., P. Parekh, B. Tilbrook, R. R. Bidigare, and E. A. Laws, 1997, Organic carbon  $\delta^{13}\text{C}$  variations in sedimentary rocks as chemostratigraphic and paleoenvironmental tools: *Palaeogeography, Palaeoclimatology, Palaeoecology*, v. 132, p. 119-132.
- Provo, L. J., R. C. Kepferle, and P. E. Potter, 1978, Division of black Ohio Shale in eastern Kentucky: *American Association of Petroleum Geologists Bulletin*, v. 62, p. 1703-1713.
- Quan, T. M., E. N. Adigwe, N. Riedinger, and J. Puckette, 2013, Evaluating nitrogen isotopes as proxies for depositional environmental conditions in shales: Comparing Caney and Woodford Shales in the Arkoma Basin, Oklahoma: *Chemical Geology*, v. 360–361, p. 231-240.
- Quan, T. M., and P. G. Falkowski, 2009, Redox control of N:P ratios in aquatic ecosystems: *Geobiology*, v. 7, p. 124-39.
- Quan, T. M., B. van de Schootbrugge, M. P. Field, Y. Rosenthal, and P. G. Falkowski, 2008, Nitrogen isotope and trace metal analyses from the Mingolsheim core (Germany): Evidence for redox variations across the Triassic-Jurassic boundary: *Global Biogeochemical Cycles*, v. 22, p. GB2014.
- Rau, G. H., M. A. Arthur, and W. E. Dean, 1987,  $^{15}\text{N}/^{14}\text{N}$  variations in Cretaceous Atlantic sedimentary sequences: implication for past changes in marine nitrogen biogeochemistry: *Earth and Planetary Science Letters*, v. 82, p. 269-279.



- Repetski, J. E., R. T. Ryder, D. J. Weary, A. G. Harris, and M. H. Trippi, 2008, Thermal maturity patterns (CAI and %R<sub>o</sub>) in Upper Ordovician and Devonian rocks of the Appalachian basin: A major revision of USGS Map I-917-E using new subsurface collections: *USGS Scientific Investigations Map 3006*, p. 26.
- Rich, J. L., 1951, Probable fondo origin of Marcellus-Ohio-New Albany-Chattanooga bituminous shales: *American Association of Petroleum Geologists Bulletin*, v. 35, p. 2017-2040.
- Rigby, D., and B. D. Batts, 1986, The isotopic composition of nitrogen in Australian coals and oil shales: *Chemical Geology: Isotope Geoscience section*, v. 58, p. 273-282.
- Rimmer, S. M., 2004, Geochemical paleoredox indicators in Devonian–Mississippian black shales, Central Appalachian Basin (USA): *Chemical Geology*, v. 206, p. 373-391.
- Rimmer, S. M., D. J. Cantrell, and P. J. Gooding, 1993, Rock-eval pyrolysis and vitrinite reflectance trends in the Cleveland Shale Member of the Ohio Shale, eastern Kentucky: *Organic Geochemistry*, v. 20, p. 735-745.
- Rimmer, S. M., J. A. Thompson, S. A. Goodnight, and T. L. Robl, 2004, Multiple controls on the preservation of organic matter in Devonian–Mississippian marine black shales: geochemical and petrographic evidence: *Palaeogeography, Palaeoclimatology, Palaeoecology*, v. 215, p. 125-154.
- Rivera, K. T., J. Puckette, and T. M. Quan, 2015, Evaluation of redox versus thermal maturity controls on  $\delta^{15}\text{N}$  in organic rich shales: A case study of the Woodford

- Shale, Anadarko Basin, Oklahoma, USA: *Organic Geochemistry*, v. 83–84, p. 127-139.
- Robinson, R. S., M. Kienast, A. Luiza Albuquerque, M. Altabet, S. Contreras, R. De Pol Holz, N. Dubois, R. Francois, E. Galbraith, T.-C. Hsu, T. Ivanochko, S. Jaccard, S.-J. Kao, T. Kiefer, S. Kienast, M. Lehmann, P. Martinez, M. McCarthy, J. Möbius, T. Pedersen, T. M. Quan, E. Ryabenko, A. Schmittner, R. Schneider, A. Schneider-Mor, M. Shigemitsu, D. Sinclair, C. Somes, A. Studer, R. Thunell, and J.-Y. Yang, 2012, A review of nitrogen isotopic alteration in marine sediments: *Paleoceanography*, v. 27, p. PA4203.
- Robl, T. L., and L. S. Barron, 1988, The geochemistry of Devonian black shales in central Kentucky and its relationship to inter-basinal correlation and depositional environment: *Devonian of the World: Proceedings of the 2nd International Symposium on the Devonian System — Memoir 14*, v. II: Sedimentation, p. 377-392.
- Roen, J. B., 1980, Stratigraphy of the Devonian Chattanooga and Ohio Shales and Equivalents in the Appalachian Basin: An Example of Long-range Subsurface Correlation Using Gamma-ray Logs, Morgantown, West Virginia, West Virginia Geological and Economic Survey, p. 26.
- Roen, J. B., 1984, Geology of the Devonian black shales of the Appalachian Basin: *Organic Geochemistry*, v. 5, p. 241-254.
- Ryder, R., P. Hackley, M. Trippi, and H. Alimi, 2013, Evaluation of thermal maturity in the low maturity Devonian shales of the northern Appalachian Basin: *AAPG Search and Discovery Article*, v. 10477.

- Sageman, B. B., A. E. Murphy, J. P. Werne, C. A. Ver Straeten, D. J. Hollander, and T. W. Lyons, 2003, A tale of shales: the relative roles of production, decomposition, and dilution in the accumulation of organic-rich strata, Middle–Upper Devonian, Appalachian basin: *Chemical Geology*, v. 195, p. 229-273.
- Schimmelmann, A., and G. P. Lis, 2010, Nitrogen isotopic exchange during maturation of organic matter: *Organic Geochemistry*, v. 41, p. 63-70.
- Schmoker, J. W., 1981, Determination of organic-matter content of Appalachian Devonian shales from gamma-ray logs: *American Association of Petroleum Geologists Bulletin*, v. 65, p. 1285-1298.
- Schroeder, P. A., and E. D. Ingall, 1994, A Method for the Determination of Nitrogen in Clays, with Application to the Burial Diagenesis of Shales: Research Method Paper: *Journal of Sedimentary Research*, v. 64A: Sedimentary Petrology and Processes, p. 694-697.
- Schubert, C. J., and S. E. Calvert, 2001, Nitrogen and carbon isotopic composition of marine and terrestrial organic matter in Arctic Ocean sediments:: implications for nutrient utilization and organic matter composition: *Deep Sea Research Part I: Oceanographic Research Papers*, v. 48, p. 789-810.
- Schwietering, J. F., 1979, Devonian shales of Ohio and their eastern and southern equivalents, Morgantown, West Virginia West Virginia Geological and Economic Survey, p. 72.
- Silva, J. A., and J. M. Bremner, 1966, Determination and Isotope-Ratio Analysis of Different Forms of Nitrogen in Soils: 5. Fixed Ammonium<sup>1</sup>: *Soil Science Society of America Journal*, v. 30, p. 587-594.

- Tassell, J. V., 1987, Upper Devonian Catskill Delta margin cyclic sedimentation: Brallier, Scherr, and Foreknobs Formations of Virginia and West Virginia: *Geological Society of America Bulletin*, v. 99, p. 414-426.
- Teske, A., E. Alm, J. M. Regan, S. Toze, B. E. Rittmann, and D. A. Stahl, 1994, Evolutionary relationships among ammonia- and nitrite-oxidizing bacteria: *Journal of Bacteriology*, v. 176, p. 6623-6630.
- Tuite Jr., M. L., 2012, The Nitrogen Biogeochemistry of Devonian Black Shale-Forming Ecosystems: Dissertation thesis, University of Virginia, Charlottesville, ProQuest, UMI Dissertations Publishing.
- Vandenbroucke, M., and C. Largeau, 2007, Kerogen origin, evolution and structure: *Organic Geochemistry*, v. 38, p. 719-833.
- Wada, E., 1980, Nitrogen isotope fractionation and its significance in biogeochemical processes occurring in marine environments, in E. D. Goldberg, Y. Horibe, and K. Saruhashi, eds., *Isotope Marine Chemistry*: Tokyo, Uchida Rokkakudo, p. 375-398.
- Wada, E., and A. Hattori, 1976, Natural abundance of  $^{15}\text{N}$  in particulate organic matter in the North Pacific Ocean: *Geochimica et Cosmochimica Acta*, v. 40, p. 249-251.
- Wada, E., T. Kadonaga, and S. Matsuo, 1975,  $^{15}\text{N}$  abundance in nitrogen of naturally occurring substances and global assessment of denitrification from isotopic viewpoint: *Geochemical Journal*, v. 9, p. 139-148.
- Ward, B. B., 2008, Chapter 5 - Nitrification in Marine Systems, in D. G. Capone, D. A. Bronk, M. R. Mulholland, and E. J. Carpenter, eds., *Nitrogen in the Marine Environment* (2nd Edition): San Diego, Academic Press, p. 199-261.

- Werne, J. P., B. B. Sageman, T. W. Lyons, and D. J. Hollander, 2002, An integrated assessment of a “type euxinic” deposit: Evidence for multiple controls on black shale deposition in the middle Devonian Oatka Creek formation: *American Journal of Science*, v. 302, p. 110-143.
- Williams, L. B., 1991, Ammonium Substitution in Illite During Maturation of Organic Matter: *Clays and Clay Minerals*, v. 39, p. 400-408.
- Williams, L. B., R. E. Ferrell Jr, E. W. Chinn, and R. Sassen, 1989, Fixed-ammonium in clays associated with crude oils: *Applied Geochemistry*, v. 4, p. 605-616.
- Williams, L. B., R. E. Ferrell Jr, I. Hutcheon, A. J. Bakel, M. M. Walsh, and H. R. Krouse, 1995, Nitrogen isotope geochemistry of organic matter and minerals during diagenesis and hydrocarbon migration: *Geochimica et Cosmochimica Acta*, v. 59, p. 765-779.
- Williams, L. B., B. R. Wilcoxon, R. E. Ferrell, and R. Sassen, 1992, Diagenesis of ammonium during hydrocarbon maturation and migration, Wilcox Group, Louisiana, U.S.A: *Applied Geochemistry*, v. 7, p. 123-134.
- Wu, L. M., C. H. Zhou, J. Keeling, D. S. Tong, and W. H. Yu, 2012, Towards an understanding of the role of clay minerals in crude oil formation, migration and accumulation: *Earth-Science Reviews*, v. 115, p. 373-386.
- Zheng, Y., R. F. Anderson, A. van Geen, and M. Q. Fleisher, 2002, Remobilization of authigenic uranium in marine sediments by bioturbation: *Geochimica et Cosmochimica Acta*, v. 66, p. 1759-1772.

## APPENDIX I

Geochemical values for bulk nitrogen isotope ( $\delta^{15}\text{N}_{\text{bulk}}$ ), inorganic nitrogen isotope ( $\delta^{15}\text{N}_{\text{inorganic}}$ ), organic carbon isotope ( $\delta^{13}\text{C}_{\text{org}}$ ), total organic carbon (TOC), inorganic nitrogen (IN), and  $\text{C}_{\text{org}}/\text{TN}$  profiles for the individual members of the Ohio Shale

DEPTH (FT)	Member	$\delta^{15}\text{N}_{\text{bulk}}$ (‰)	$\delta^{15}\text{N}_{\text{inorg}}$ (‰)	TN (wt %)	IN (wt %)	$\delta^{13}\text{C}_{\text{org}}$ (‰)	TOC (wt %)	$\text{C}_{\text{org}}/\text{TN}$
2850	Clvd Eq	0.9	1.2	1.7	1.3	-28.8	5.8	3.4
2860	Clvd Eq	1.2	1.6	1.9	1.7	-28.8	9.4	4.9
2870	Clvd Eq	1.5	1.0	1.4	1.1	-28.4	5.7	4.2
2880	Clvd Eq	1.6	1.2	1.3	1.0	*	5.8	4.3
2890	Clvd Eq	1.4	1.2	1.6	1.4	-28.9	7.8	4.9
2900	Clvd Eq	1.1	0.6	1.7	1.3	-29.0	5.6	3.4
2910	Clvd Eq	0.5	0.5	1.2	1.0	-28.2	4.7	3.8
2920	Clvd Eq	0.8	0.5	1.2	1.0	-28.4	4.1	3.3
2930	Chagrin	0.8	0.0	1.2	1.0	-27.9	2.1	1.7
2940	Chagrin	0.3	-0.2	0.9	0.7	*	0.6	0.7
2950	Chagrin	0.2	-0.1	0.9	0.8	-25.3	0.5	0.6
2960	Chagrin	0.1	-0.3	1.0	0.8	-24.8	0.4	0.4
2970	Chagrin	0.0	-0.2	1.0	0.8	-25.0	0.4	0.4
2980	Chagrin	0.1	-0.4	1.2	1.0	-28.0	1.4	1.2
2990	Chagrin	0.1	-0.4	1.2	1.0	-28.5	1.9	1.7
3000	Chagrin	-1.9	-0.6	1.4	1.1	-28.4	1.8	1.3
3010	Chagrin	0.0	-0.3	1.2	1.0	-26.9	0.9	0.7
3020	Chagrin	-0.2	-0.5	0.9	0.9	-25.8	0.4	0.5
3030	Chagrin	-0.3	-0.3	1.0	0.9	-26.3	0.5	0.5
3040	Chagrin	-0.3	-0.4	0.9	0.9	-25.4	0.4	0.4
3050	Chagrin	-0.3	-0.4	1.0	0.9	-25.8	0.3	0.3
3060	Chagrin	-0.1	-0.3	1.1	0.9	-25.2	0.4	0.3
3070	Chagrin	-0.3	-0.3	0.9	0.9	-25.5	0.4	0.4
3080	U Huron	-1.9	-0.8	1.5	1.2	-27.6	2.6	1.8
3090	U Huron	-1.3	-1.1	1.5	1.2	-27.8	2.6	1.7
3100	U Huron	-1.4	-1.1	1.5	1.2	-28.6	3.2	2.1
3110	U Huron	-1.2	-1.0	1.7	1.3	*	3.6	2.1
3120	U Huron	-1.1	-0.9	1.6	1.3	-28.7	3.8	2.4
3130	M Huron	-1.2	-1.2	1.4	1.2	-27.9	2.1	1.5
3140	M Huron	-1.6	-1.1	1.4	1.1	-29.0	2.2	1.6
3150	M Huron	-1.5	-0.9	1.4	1.0	*	2.0	1.4
3160	M Huron	-1.8	-0.8	1.3	1.1	-28.2	2.0	1.5
3170	M Huron	-0.6	-0.8	1.3	1.1	-26.1	0.7	0.5
3180	M Huron	-0.9	-0.7	1.4	1.2	-27.6	0.9	0.6
3190	M Huron	-1.3	-0.9	1.3	1.1	-27.9	0.9	0.7

DEPTH (FT)	Member	$\delta^{15}\text{N}_{\text{bulk}}$ (‰)	$\delta^{15}\text{N}_{\text{inorg}}$ (‰)	TN (wt %)	IN (wt %)	$\delta^{13}\text{C}_{\text{org}}$ (‰)	TOC (wt %)	$\text{C}_{\text{org}}/\text{TN}$
3200	M Huron	-0.8	-0.9	1.3	1.0	-26.8	0.7	0.6
3210	M Huron	-0.2	-0.7	1.3	1.0	-25.4	0.6	0.5
3220	M Huron	-0.5	-0.9	1.3	1.1	-25.6	0.6	0.5
3230	M Huron	-0.5	-0.8	1.30	0.98	-25.2	0.49	0.37
3240	M Huron	-0.7	-0.7	1.33	1.25	-26.9	0.55	0.41
3250	M Huron	-0.7	-0.9	1.07	1.25	-25.8	0.52	0.48
3260	M Huron	-1.6	-1.2	1.50	1.38	-28.6	2.09	1.39
3270	M Huron	-1.2	-1.1	1.41	1.28	-27.1	1.02	0.72
3280	M Huron	-1.0	-1.0	1.37	1.24	-27.4	0.67	0.49
3290	M Huron	-0.7	-0.9	1.37	1.32	-28.6	1.39	1.01
3300	M Huron	-1.1	-1.0	1.53	1.42	*	1.83	1.20
3310	M Huron	-1.4	-1.2	1.41	1.40	-29.1	2.13	1.51
3320	M Huron	-1.9	-1.3	1.50	1.38	*	4.23	2.82
3330	M Huron	-2.3	-1.6	1.51	1.48	-29.6	4.11	2.73
3340	M Huron	-1.9	-1.4	1.56	1.43	-29.7	4.40	2.82
3350	M Huron	-0.7	-1.1	1.48	1.38	-28.4	1.01	0.68
3360	M Huron	-0.7	-1.1	1.35	1.42	-27.9	0.62	0.46
3370	M Huron	-1.1	-1.0	1.22	1.30	-28.8	0.58	0.48
3380	M Huron	-0.8	-1.0	1.35	1.32	-25.4	0.59	0.44
3390	L Huron	-2.5	-1.9	1.75	1.71	-30.0	7.11	4.07
3400	L Huron	-1.6	-1.6	1.76	1.65	-30.3	6.76	3.84
3410	L Huron	-1.4	-1.5	1.84	1.71	-30.3	6.57	3.57
3420	L Huron	-1.6	-1.5	1.78	1.57	-30.5	4.81	2.70
3430	L Huron	-1.3	-1.8	1.59	1.41	-30.3	4.08	2.57
3450	L Huron	-1.5	-1.7	1.68	1.45	-30.6	4.59	2.73
3460	L Huron	-1.2	-1.6	1.71	1.63	-30.2	5.47	3.19
3470	L Huron	-2.0	-2.1	1.85	1.70	-30.2	4.79	2.59
3480	L Huron	-1.7	-1.7	1.71	1.68	-29.9	5.75	3.36
3490	L Huron	-2.3	-1.9	1.66	1.52	-29.9	5.08	3.06
3500	L Huron	-2.1	-1.6	1.70	1.34	-29.8	5.50	3.23
3510	L Huron	-2.3	-1.9	1.69	1.57	-29.6	5.54	3.28
3520	L Huron	-1.6	-1.7	1.60	1.50	-29.9	3.80	2.38
3530	L Huron	-2.1	-2.0	1.74	1.83	-29.1	9.31	5.36

\* denotes that measurements were not collected due to machine error; therefore,  $\delta^{13}\text{C}_{\text{org}}$  averages and standard deviations for individual members are associated with some statistical error, but are assumed to be minimal

## APPENDIX II

Munsell color indices for individual members of the Ohio Shale.

DEPTH (FT)	Member	Hue	Value/ Chroma	Color
<b>2850</b>	Clvd Eq	7.5 YR	4/1	dark gray
<b>2860</b>	Clvd Eq	7.5 YR	3/1	very dark gray
<b>2870</b>	Clvd Eq	7.5 YR	4/1	dark gray
<b>2880</b>	Clvd Eq	7.5 YR	4/1	dark gray
<b>2890</b>	Clvd Eq	7.5 YR	4/1	dark gray
<b>2900</b>	Clvd Eq	7.5 YR	4/1	dark gray
<b>2910</b>	Clvd Eq	7.5 YR	4/1	dark gray
<b>2920</b>	Clvd Eq	7.5 YR	4/1	dark gray
<b>2930</b>	Chagrin	7.5 YR	5/1	gray
<b>2940</b>	Chagrin	5 YR	7/1	light gray
<b>2950</b>	Chagrin	5 YR	7/1	light gray
<b>2960</b>	Chagrin	5 YR	7/1	light gray
<b>2970</b>	Chagrin	5 YR	7/1	light gray
<b>2980</b>	Chagrin	5 YR	6/1	gray
<b>2990</b>	Chagrin	5 YR	6/1	gray
<b>3000</b>	Chagrin	5 YR	6/1	gray
<b>3010</b>	Chagrin	5 YR	6/1	gray
<b>3020</b>	Chagrin	5 YR	7/1	light gray
<b>3030</b>	Chagrin	5 YR	7/1	light gray
<b>3040</b>	Chagrin	5 YR	7/1	light gray
<b>3050</b>	Chagrin	5 YR	7/1	light gray
<b>3060</b>	Chagrin	5 YR	7/1	light gray
<b>3070</b>	Chagrin	5 YR	7/1	light gray
<b>3080</b>	U Huron	7.5 YR	5/1	gray
<b>3090</b>	U Huron	7.5 YR	5/1	gray
<b>3100</b>	U Huron	7.5 YR	4/1	dark gray
<b>3110</b>	U Huron	7.5 YR	4/1	dark gray
<b>3120</b>	U Huron	7.5 YR	4/1	dark gray
<b>3130</b>	M Huron	7.5 YR	5/1	gray
<b>3140</b>	M Huron	7.5 YR	5/1	gray
<b>3150</b>	M Huron	7.5 YR	5/1	gray
<b>3160</b>	M Huron	7.5 YR	5/1	gray
<b>3170</b>	M Huron	7.5 YR	6/2	pinkish gray
<b>3180</b>	M Huron	7.5 YR	6/1	gray
<b>3190</b>	M Huron	7.5 YR	6/1	gray



DEPTH (FT)	Member	Hue	Value/ Chroma	Color
3200	M Huron	7.5 YR	6/1	gray
3210	M Huron	7.5 YR	6/1	gray
3220	M Huron	7.5 YR	6/2	pinkish gray
3230	M Huron	7.5 YR	6/1	gray
3240	M Huron	7.5 YR	6/1	gray
3250	M Huron	7.5 YR	6/1	gray
3260	M Huron	7.5 YR	5/1	gray
3270	M Huron	7.5 YR	6/1	gray
3280	M Huron	7.5 YR	6/1	gray
3290	M Huron	7.5 YR	6/1	gray
3300	M Huron	7.5 YR	5/1	gray
3310	M Huron	7.5 YR	5/1	gray
3320	M Huron	7.5 YR	5/1	gray
3330	M Huron	7.5 YR	4/1	dark gray
3340	M Huron	7.5 YR	4/1	dark gray
3350	M Huron	7.5 YR	6/1	gray
3360	M Huron	7.5 YR	6/1	gray
3370	M Huron	7.5 YR	6/1	gray
3380	M Huron	7.5 YR	6/1	gray
3390	L Huron	7.5 YR	4/1	dark gray
3400	L Huron	7.5 YR	3/2	dark brown
3410	L Huron	7.5 YR	3/2	dark brown
3420	L Huron	7.5 YR	4/1	dark gray
3430	L Huron	7.5 YR	4/2	brown
3450	L Huron	7.5 YR	3/1	very dark gray
3460	L Huron	7.5 YR	4/2	brown
3470	L Huron	7.5 YR	3/2	dark brown
3480	L Huron	7.5 YR	4/2	brown
3490	L Huron	7.5 YR	4/2	brown
3500	L Huron	7.5 YR	3/1	very dark gray
3510	L Huron	7.5 YR	3/1	very dark gray
3520	L Huron	7.5 YR	4/1	dark gray
3530	L Huron	7.5 YR	2.5/1	black

VITA

Brice Aaron Otto

Candidate for the Degree of

Master of Science

Thesis: CHARACTERIZATION OF DEVONIAN BLACK SHALE DEPOSITIONAL ENVIRONMENTS AND DIAGENETIC/CATAGENETIC PROCESSES USING NITROGEN ISOTOPES AND OTHER GEOCHEMICAL PROXIES: OHIO SHALE, EASTERN KENTUCKY

Major Field: Geology

Biographical:

Education:

Completed the requirements for the Master of Science in Geology at Oklahoma State University, Stillwater, Oklahoma in July, 2015.

Completed the requirements for the Bachelor of Science in Geology at the University of Tulsa, Tulsa, Oklahoma in 2013.

Experience:

SM Energy, Tulsa, OK, Geoscientist Intern from May 2014 to August 2014.

Baker Hughes, Oklahoma City, OK, Reservoir Navigation Specialist Intern from May 2012 to August 2012.

Mustang Fuel Corporation, Oklahoma City, OK, Geology Technician Intern from May 2011 to August 2011.

Professional Memberships:

American Association of Petroleum Geologists  
Geological Society of America  
Geochemical Society